

FedST: Secure Federated Shapelet Transformation for Time Series Classification

Zhiyu Liang · Hongzhi Wang

Received: date / Accepted: date

Abstract This paper explores how to customize time series classification (TSC) methods with the help of external data in a privacy-preserving federated learning (FL) scenario. To the best of our knowledge, we are the first to study on this essential topic. Achieving this goal requires us to seamlessly integrate the techniques from multiple fields including Data Mining, Machine Learning, and Security. In this paper, we systematically investigate existing TSC solutions for the centralized scenario and propose FedST, a novel FL-enabled TSC framework based on a shapelet transformation method. We recognize the federated shapelet search step as the kernel of FedST. Thus, we design a basic protocol for the FedST kernel that we prove to be secure and accurate. However, we identify that the basic protocol suffers from efficiency bottlenecks and the centralized acceleration techniques lose their efficacy due to the security issues. To speed up the federated protocol with security guarantee, we propose several optimizations tailored for the FL setting. Our theoretical analysis shows that the proposed methods are secure and more efficient. We conduct extensive experiments using both synthetic and real-world datasets. Empirical results show that our FedST solution is effective in terms of TSC accuracy, and the proposed optimizations can achieve three orders of magnitude of speedup.

Keywords Time series classification · Federated Learning · Time series features · Time series shapelets

Zhiyu Liang.
Harbin Institute of Technology, Harbin, China
E-mail: zyliang@hit.edu.cn

Hongzhi Wang.
Harbin Institute of Technology, Harbin, China
E-mail: wangzh@hit.edu.cn

1 Introduction

Time series classification (TSC) aims to predict the class label for given time series samples. It is one of the most important problem for data analytics, with applications in various scenarios [82, 24, 78].

Despite the impressive performance existing TSC algorithms have been achieving [7, 39, 2, 79, 68, 84, 22, 83], they usually make an ideal assumption that the user has free access to enough labeled data. However, it is quite difficult to collect and label the time series for real-world applications.

For instance, small manufacturing businesses monitor their production lines using sensors to analyze the working condition. Since the data sequences related to specific conditions, e.g., a potential failure of an instrument, are usually rare pieces located in unknown regions of the whole monitoring time series, the users have to manually identify the related pieces for labeling, which can be expensive due to the need of professional knowledge. As a consequence, it is costly for these businesses to benefit from the advanced TSC solutions, as they have no enough labeled data to learn accurate models.

To deal with the problem, a natural idea is to enrich the local training data by gathering the labeled samples from external data sources, e.g., the other businesses that run the same instrument. However, it has been increasingly difficult for organizations to combine their data due to privacy concerns [90, 86].

1.1 Motivation

Is it possible to develop accurate TSC methods with the help of external datasets in a privacy-preserving

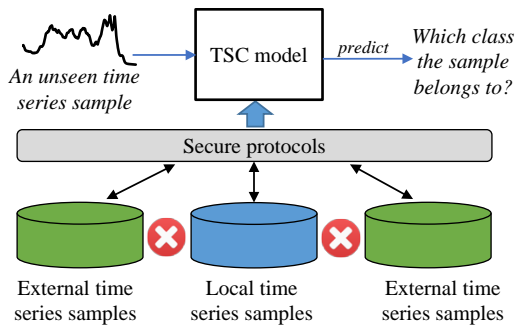


Fig. 1: Example of enabling federated learning to enrich the training time series data. A business who owns some training time series samples (blue) collaborates with the partners who have additional training samples (green) to jointly build the TSC model. They follow some secure protocols to avoid disclosing their private training data.

manner? A recent concept, named *Federated Learning* (FL) [63], provides us an inspiration [53]. FL aims to enable multiple businesses to jointly train a model without revealing their private data to each other. An example of using FL to enrich the training time series data is shown in Figure 1. However, although many FL solutions have been studied in the literature [90, 47, 95, 40, 61], their main focus is the training of the general models, including tree models [89, 29, 27, 3, 19, 48], linear models [74, 70, 16, 5, 91], and neural networks [63, 80, 65, 64, 11, 1, 30], which have limitations for the TSC problem.

First, the tree-based and linear classifiers are shown weak in capturing the temporal patterns for classifying time series [7], while the accuracy of neural networks usually relies on the hyper-parameter tuning, which is still a challenging problem in the FL scenario. Second, many real-world TSC applications [31, 93, 78, 76] expect the classification decisions to be explainable, e.g., the users know why a working condition is determined as a fault. However, the time series sample usually has a large number of data points (e.g., 537 on average for the 117 fixed-length datasets of the UCR Archive [21]), which are taken as independent variables by the general models. The explanation can be much complex with so much input variables.

Facing the above limitations, we propose to specifically design FL solutions for the TSC problem. The basic idea is to extend the customized centralized TSC approaches to the federated setting. To achieve this goal, we have proposed FedTSC [53], a brand new FL system tailored for TSC, and demonstrated its utility in VLDB. In this paper, we elaborate on the design ideas and essential techniques of a main internal of the system, i.e., the novel Federated Shapelet Transformation (FedST)

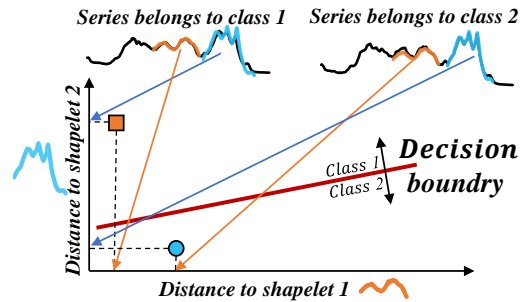


Fig. 2: Illustration of the shapelet-based features. A shapelet is a salient subsequence that represents the shape unique to certain classes. With a few shapelets of high distinguishing ability, each time series sample is transformed into a low-dimensional feature vector representing how similar (distant) the sample is to these shapelets. The classification is made and explained based on the few features rather than the abundant datapoints of the raw time series. In this example, the time series similar to shapelet 1 (orange) and distant to shapelet 2 (blue) are classified into class 1 and vice versa.

framework. We design FedST based on the centralized shapelet transformation method due to the following benefits.

First, the shapelet transformation method not only achieves competitive accuracy over existing centralized TSC approaches [7], but also serves as an essential component of the ensemble classifier named HIVE-COTE 2.0, which is currently state-of-the-art centralized TSC model [68]. Second, the method adopts the shapelet-based features rather than the raw time series as the input of the classification models. The features represent the similarity between the time series and a set of shapelets (i.e., the salient subsequences), which can be order-of-magnitude less in number compared to the raw data points and very intuitive to understand [35]. Thus, building classifiers on top of the shapelet-based features can simplify the explanation. Third, the shapelets used to transform the raw time series can be extracted in an anytime manner to flexibly balance the classification accuracy and the efficiency (see Section 4.2), which are beneficial for practical utility. Figure 2 is an illustration of the shapelet-based features.

1.2 Challenges and contributions

Although it is practical to extend the centralized approach to the federated setting, it is unexplored how to achieve both security and efficiency during the federated

ated shapelet search (FedSS) step, which is the kernel of the FedST framework (see Section 4.2 in detail).

The goal of the federated shapelet search is to jointly utilize the distributed labeled time series data to find the shapelets with the highest quality for distinguishing the classes. To ensure security of the federated computation, a natural idea is to extend the centralized shapelet search using secure multi-party computation (MPC) [92, 20, 41, 42]. Following that, we first develop $\Pi_{FedSS-B}$, the basic protocol to achieve FedSS. Benefiting from MPC, we show that this protocol is secure and effective.

However, by our analysis, the basic protocol suffers from low efficiency due to the high overhead incurred by MPC during the *shapelet distance computation* and the *shapelet quality measurement* stages. Although there are acceleration techniques in the centralized scenario [72, 43, 93, 77], we prove that these methods are insecure in the FL setting and thus to be unfeasible. Consequently, we propose acceleration methods tailored for the FL setting with security guarantee to tackle the efficiency bottlenecks of $\Pi_{FedSS-B}$.

For shapelet distance computation, we identify the Euclidean norm computation as the efficiency bottleneck, so we propose a speed-up method based on a novel secure dot-product protocol. For quality measurement, we first design an optimization to reduce the duplicated time-consuming interactive operations with secure sorting. Then, we propose to further boost the efficiency through an acceptable trade-off of classification accuracy. We show both *theoretically* and *empirically* the effectiveness of these techniques.

Contributions. We summarize our contributions as follows.

1. We investigate the customized FL solution for time series classification. In particular, we propose FedST, the first shapelet-based FL method which extends the centralized shapelet transformation to the federated scenario to make use of its advantages in terms of accuracy, interpretability and flexibility.
2. We present $\Pi_{FedSS-B}$, a basic federated protocol for the FedST kernel, i.e., the federated shapelet search, which adopts MPC to achieve security. We analyze the protocol in terms of security, effectiveness, and efficiency. We identify the efficiency bottlenecks of $\Pi_{FedSS-B}$ and the invalidity of the centralized speed-up techniques due to the security issue. To boost the protocol efficiency, we propose acceleration methods tailored for the FL setting, which are theoretically secure and are more scalable and efficient than the basic protocol.
3. We conduct extensive experiments to evaluate our solutions, which has three major observations. (1) Our FedST offers superior accuracy comparable to the non-private approach. (2) Each of our proposed acceleration approaches is individually effective, and they together bring up to three orders of magnitude of speedup. (3) The proposed trade-off method provides up to 8.31x speedup over our well-optimized protocol while guaranteeing comparable accuracy. We further demonstrate the interpretability and flexibility of our framework.

Organization. We introduce the preliminaries in Section 3. We propose the FedST framework and talk about the FedST kernel, i.e., federated shapelet search, in Section 4. The basic protocol of the federated shapelet search is presented and analyzed in Section 5. We elaborate on the acceleration methods tailored for the two efficiency bottlenecks of the basic protocol in Section 6 and 7, respectively. We show experimental results in Section 8. We illustrate how to incorporate differential privacy to further enhance the security in Section 9 and conclude this paper in Section 10.

2 Related Work

Our work is related to federated learning, feature-based time series classification, and privacy protection.

2.1 Federated Learning

Recently, there have been numerous works that dedicate to the federated learning of the general models, including the linear models [74, 70, 16, 5, 91], the tree models [89, 29, 27, 3, 19, 48], and the neural networks [63, 80, 65, 64, 11, 1, 94, 30]. However, none of them achieve the same goal as our solution, because these general models have limitations in tackling the TSC problem [7] in terms of accuracy and interpretability. There are also FL solutions designed for specific tasks [65, 57, 87, 37, 58, 51, 85, 73, 50, 17, 81]. These methods target scenarios that are completely different from ours. As a result, we propose to tailor FL method for TSC. In specific, we contribute to proposing the secure FedST framework to take advantage of the shapelet transformation in terms of accuracy, interpretability and flexibility, and addressing the security and efficiency issues within the framework.

2.2 Feature-based Time Series Classification

Instead of directly building classifiers upon the raw time series, transforming the time series into low-dimensional or sparse feature vectors can not only achieve competitive classification accuracy, but also simplify the explanation.

In summary, there are three types of TSC methods based on different explainable features, i.e., the shapelet-based methods [93, 72, 35, 12, 34, 46, 52] that determine the class labels based on the localized shapes, the interval-based methods [66, 13, 68] that classify the time series based on the statistics at some specific time ranges, and the dictionary-based approaches [45, 44, 69, 67] that utilize the pattern frequency as features. These types of methods can be complement with each other to contribute to state-of-the-art accuracy [55, 6, 68]. This work focuses on developing a novel framework with a series of optimization techniques taking advantage of the shapelet-based approaches, while we would like to present our contributions [53] of enabling FL for interval-based and dictionary-based TSC in the future.

Shapelet-based TSC is first proposed by [93]. In the early works, the shapelets are discovered in a company with a decision tree training, where a shapelet is found at each tree node to determine the best split of the node [93, 72, 54]. To benefit from the other classifiers, a shapelet transformation framework [35] is proposed that decouples the shapelet discovery from the decision tree training and produces a transformed dataset that can be used in conjunction with any classifier. Several works are raised to speedup the shapelet search [93, 43, 72, 77] and improve the shapelet quality [12].

Another line of works dedicate to jointly learning the shapelets and the classifiers [34, 52, 59, 46, 60, 28, 36]. However, the learning-based methods are much more complex because they incur several additional hyperparameters that highly affect the accuracy. Besides, they are inflexible due to the coupling of the shapelet and classifier, and cannot run in the anytime fashion to trade off the classification accuracy and the efficiency.

Based on the above discussions, we take advantage of the shapelet transformation method [35, 12, 6] to develop our FL solution. Nevertheless, our work differs from existing studies because we carefully consider the security and efficiency issues in a brand new FL scenario.

2.3 Privacy Protection

Data privacy is one of the most essential problems in FL [90, 49, 40]. Several techniques have been studied by existing works. Secure Multi-Party Computation [92]

is a general framework that offers secure protocols for many arithmetic operations [20, 41, 42]. These operations are efficient for practical utility [4, 18, 48, 70, 50, 89] under the semi-honest model that most FL works consider, while they can also be extended to the malicious model through zero-knowledge proofs [32].

Homomorphic Encryption (HE) is another popular technique in FL [19, 29, 58, 94, 89], which allows a simple implementation of the secure addition. However, HE does not support some complex operations (e.g., division and comparison). The encryption and decryption are also computationally intensive [89, 29].

Compared to the solutions based on MPC and HE which aim to protect the intermediate information during the federated computation, an orthogonal line of works adopt the Differential Privacy (DP) to protect the privacy for the outputs, such as the parameters of the learned models. It works by adding noises to the private data [87, 88, 56, 51, 75] to achieve a trade-off between the precision and the degree of privacy for a target function. Thus, DP can usually complement with MPC and HE.

In this paper, we mainly adopt MPC to ensure no intermediate information is disclosed during the complex computations of FedST, because it provides the protocols for the required arithmetic operations. We also illustrate that the private data can be further protected with privacy guarantee by incorporating DP.

3 Preliminaries

This section presents the preliminaries, including the target problem of the paper and the two building blocks of the proposed FedST, i.e., the shapelet transformation and the secure multi-party computation.

3.1 Problem Statement

Time series classification (TSC) is the problem of creating a function that maps from the space of input time series samples to the space of class labels [7]. A time series (sample) is defined as a sequence of data points $T = (t_1, \dots, t_p, \dots, t_N)$ ordered by time, where t_p is the observation at timestamp p , and N is the length. The class label y is a discrete variable with C possible values. i.e., $y \in \{c\}_{c=1}^C$ where $C \geq 2$.

Typically, TSC is achieved by using a training data set $TD = \{(T_j, y_j)\}_{j=1}^M$ to build a model that can output either predicted class values or class distributions for previously unseen time series samples, where the instance (T_j, y_j) represents the pair of the j -th time series sample and the corresponding label.

Specifically, in this paper we target the TSC problem in a federated setting, denoted as the FL-enabled TSC problem defined as follows.

Definition 1 (FL-enabled TSC problem) Given a party P_0 (named initiator) who owns a training data set TD^0 and $n - 1$ partners P_1, \dots, P_{n-1} (named participants) who hold the labeled series TD^1, \dots, TD^{n-1} collected from the same area (e.g., monitoring the same type of instruments), where $TD^i = \{(T_j^i, y_j^i)\}_{j=1}^{M_i}$, the goal of the problem is to coordinate the parties to build TSC models \mathcal{M} for the initiator P_0 without revealing the local data TD^0, \dots, TD^{n-1} to each other.

Note that every party in the group can act as the initiator to benefit from the federated learning. For ease of exposition, we denote $\sum_{i=0}^{n-1} M_i = M$ and $\bigcup_{i=0}^{n-1} TD^i = TD$. Ideally, the performance of \mathcal{M} should be lossless compared to that of the model trained in a centralized scenario using the combined data TD .

Similar to previous FL works [89, 29, 30, 51, 85], we consider the semi-honest model where each party follows the protocols but may try to infer the private information from the received messages, while our method can be extended to the malicious model through zero-knowledge proofs [32]. Unlike existing FL works that usually conditionally allow disclosure of some private data [29, 58], we adopt a stricter security definition [89, 70] to ensure *no intermediate information is disclosed*.

Definition 2 (Security) Let \mathcal{F} be an *ideal* functionality such that the parties send their data to a trusted party for computation and receive the final results from the party. Let Π be a *real-world* protocol executed by the parties. We say that Π securely realizes \mathcal{F} if for each adversary \mathcal{A} attacking the real interaction, there exists a simulator \mathcal{S} attacking the ideal interaction, such that for all environments \mathcal{Z} , the quantity $|\Pr[REAL(\mathcal{Z}, \mathcal{A}, \Pi, \lambda) = 1] - \Pr[IDEAL(\mathcal{Z}, \mathcal{S}, \mathcal{F}, \lambda) = 1]|$ is negligible (in λ).

Intuitively, the simulator \mathcal{S} must achieve the same effect in the ideal interaction as the adversary \mathcal{A} achieves in the real interaction. In this paper, we identify the ideal functionality as the federated search of the high-quality shapelets, which is the kernel of the proposed FedST framework (see Section 4.2 in detail). Therefore, we contribute to design secure and efficient protocols to achieve the functionality in the real FL scenario.

The federated setting in this paper is similar to the horizontal and cross-silo FL [40, 61] because the data are horizontally partitioned across a few businesses and each of them has considerable but insufficient data. However, unlike the mainstream FL solutions that usually rely on a trust server [37, 94, 62], we remove this

dependency considering that identifying such a party can cause additional costs [58]. Besides, the security definition we adopt is stricter than many existing FL works as mentioned above. Therefore, our setting can be more practical but challenging.

3.2 Shapelet Transformation

Time series shapelets are defined as representative subsequences that discriminate the classes. Denote $S = (s_1, \dots, s_L)$ a shapelet generated from $TD = \{(T_j, y_j)\}_{j=1}^M$ and the length of T_j is N , where $L \leq N$. Let $T_j[s, l]$ denote the subseries of $T_j = (t_{j,1}, \dots, t_{j,N})$ that starts at the timestamp s and has length l , i.e.,

$$T_j[s, l] = (t_{j,s}, \dots, t_{j,s+l-1}), 1 \leq s \leq N - l + 1, \quad (1)$$

the distance between the shapelet and the j -th time series is defined as the minimum Euclidean norm (ignore the square root) between S and the L -length subseries of T_j , i.e.,

$$d_{T_j, S} = \min_{p \in \{1, \dots, N-L+1\}} \|S - T_j[p, L]\|^2. \quad (2)$$

By definition, $d_{T_j, S}$ reflects the similarity between a localized shape of T_j and S , which is a class-specific feature. The quality of S can be measured by computing the distances to all series in TD , i.e., $D_S = \{d_{T_j, S}\}_{j=1}^M$, and evaluating the differences in distribution of the distances between class values $\{y_j\}_{j=1}^M$. The state-of-the-art method of shapelet quality measurement is to use the *Information Gain (IG) with a binary strategy* [12]. Each distance $d_{T_j, S} \in D_S$ is considered as a splitting threshold, denoted as τ . The threshold is used to partition the dataset D_S into $D_S^{\tau, L}$ and $D_S^{\tau, R}$, such that $D_S^{\tau, L} = \{d_{T_j, S} | d_{T_j, S} \leq \tau\}_{j=1}^M$ and $D_S^{\tau, R} = D_S \setminus D_S^{\tau, L}$. The quality of S is the maximum information gain among the thresholds, i.e.,

$$Q_{IG}(S) = \max_{\forall \tau} H(D_S) - (H(D_S^{\tau, L}) + H(D_S^{\tau, R})), \quad (3)$$

where

$$H(D) = -(p \log_2 p + (1 - p) \log_2 (1 - p)), \quad (4)$$

$p = \frac{|D_{y(S)}|}{|D|}$ is the fraction of samples in D that belongs to the class of the sample generating S , $y(S) \in \{c\}_{c=1}^C$ and $D_{y(S)} = \{d_{T_j, S} | y_j = y(S)\}_{j=1}^M$.

In shapelet transformation, a set of candidates are randomly sampled from the possible subsequences of TD . After measuring the quality of all candidates, the K subsequences with the highest quality are chosen as the shapelets, which are denoted as $\{S_k\}_{k=1}^K$. The

shapelets are used to transform the original dataset TD into a newly tabular dataset of K features, where each attribute represents the distance between the shapelet and the original series, i.e., $D = \{(\mathbf{X}_j, y_j)\}_{j=1}^M$ where $\mathbf{X}_j = (d_{T_j, S_1}, \dots, d_{T_j, S_K})$. The unseen series are transformed in the same way for prediction. D can be used in conjunction with any classifier, such as the well-known intrinsically interpretable decision tree and logistic regression [71].

3.3 Secure Multiparty Computation

Secure multiparty computation (MPC) [92] allows participants to compute a function over their inputs while keeping the inputs private. In this paper, we utilize the additive secret sharing scheme for MPC [20] since it offers the protocols of the common arithmetic operations applicable to practical situations [18, 50]. It performs in a field \mathbb{Z}_q for a prime q . We denote a value $x \in \mathbb{Z}_q$ that is additively shared among parties as

$$\langle x \rangle = \{\langle x \rangle_0, \dots, \langle x \rangle_{n-1}\}, \quad (5)$$

where $\langle x \rangle_i$ is a random *share* of x hold by party P_i .

Suppose x is a private value of P_i . To secretly share x , P_i randomly chooses $\langle x \rangle_j \in \mathbb{Z}_q$ and sends it to $P_j (j \neq i)$. Then, P_i sets $\langle x \rangle_i = x - \sum_{j \neq i} \langle x \rangle_j \pmod q$. To reconstruct x , all parties reveal their *shares* to compute $x = \sum_{i=0}^{n-1} \langle x \rangle_i \pmod q$. For ease of exposition, we omit the modular operation in the rest of the paper.

Under the additive secret sharing scheme, a function $z = f(x, y)$ is computed by using a MPC protocol that takes $\langle x \rangle$ and $\langle y \rangle$ as input and outputs the secret shared $\langle z \rangle$. In this paper, we mainly use the following MPC protocols as building blocks:

- (a) *Addition*: $\langle z \rangle = \langle x \rangle + \langle y \rangle$
- (b) *Multiplication*: $\langle z \rangle = \langle x \rangle \cdot \langle y \rangle$
- (c) *Division*: $\langle z \rangle = \langle x \rangle / \langle y \rangle$
- (d) *Comparison*: $\langle z \rangle = \langle x \rangle \stackrel{?}{<} \langle y \rangle : \langle 1 \rangle : \langle 0 \rangle$
- (e) *Logarithm*: $\langle z \rangle = \log_2(\langle x \rangle)$

We refer readers to [9, 15, 14, 4] for the detailed implementation of the operations.

In addition, given the result $\langle b \rangle = \langle x \rangle \stackrel{?}{<} \langle y \rangle : \langle 1 \rangle : \langle 0 \rangle$, the smaller one of two values $\langle x \rangle, \langle y \rangle$ can be securely assigned to $\langle z \rangle$, as:

- (f) *Assignment*: $\langle z \rangle = \langle b \rangle \cdot \langle x \rangle + (1 - \langle b \rangle) \cdot \langle y \rangle$.

With the assignment protocol, it is trivial to perform the *maximum*, *minimum*, and *top-K* computation for a list of secret shares by sequentially comparing and swapping the adjacent elements in the list using the secure comparison and assignment protocols.

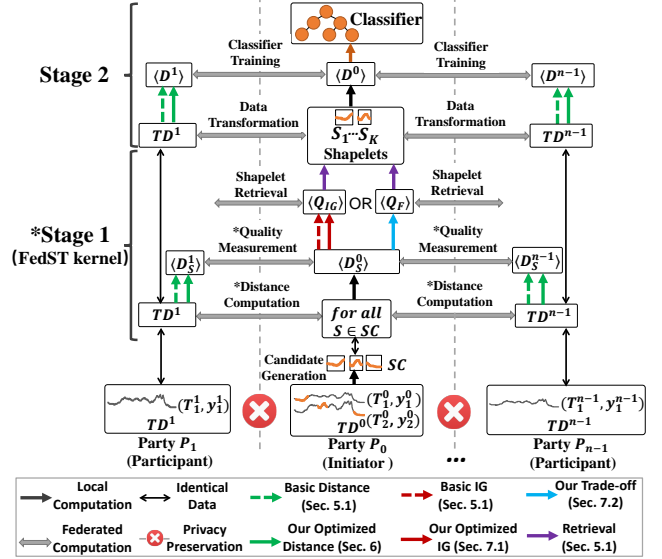


Fig. 3: An illustration of the FedST framework.

4 Solution Overview

This section overviews our FL-enabled TSC framework, which is a key component of our FedTSC system [53] and is built based on the centralized shapelet transformation [35, 12, 6]. We provide the framework overview in Section 4.1. Then, we identify the FedST kernel in Section 4.2.

4.1 FedST Framework

Overall, FedST has two stages: (1) federated shapelet search; (2) federated data transformation and classifier training. The two stages are illustrated in Figure 3.

In the first stage, all parties jointly search for the K best shapelets $\{S_k\}_{k=1}^K$ from a candidate set \mathcal{SC} .

Note that P_0 requires the found shapelets to explain the shapelet-based features, so the shapelet candidates in \mathcal{SC} are only generated by P_0 to ensure the local time series of the participants cannot be accessed by the initiator. This may raise a concern that the shapelets will be missed if they do not occur in TD_0 . Fortunately, since the high-quality shapelets are usually highly redundant in the training data, it is shown enough to find them by checking some randomly sampled candidates rather than all possible subsequences [6, 33]. Hence, it is feasible to generate \mathcal{SC} by P_0 in our cross-silo setting where each business has considerable (but insufficient) data. We also verify this issue in Section 8.2 and 8.5.

In stage two, the time series data TD^i in each party is transformed into the K dimensional secretly shared

tabular data as:

$$\langle D^i \rangle = \{(\langle \mathbf{X}_j^i \rangle, \langle y_j^i \rangle)\}_{j=1}^{M_i}, \forall i \in \{0, \dots, n-1\}, \quad (6)$$

where

$$\langle \mathbf{X}_j^i \rangle = (\langle d_{T_j^i, S_1} \rangle, \dots, \langle d_{T_j^i, S_K} \rangle). \quad (7)$$

Then, a standard classifier is built over the joint secretly shared data set $\langle D \rangle = \bigcup_{i=0}^{n-1} \langle D^i \rangle$.

Note that there is always a trade-off between security and accuracy/interpretability in FL. To achieve a good balance, FedST ensures only P_0 learns the shapelets and classifiers, while nothing else can be revealed to the parties. This degree of privacy has been shown practical by many FL systems [29, 30, 89]. Additionally, we illustrate in Section 9 that we can further enhance the security by incorporating differential privacy [26], guaranteeing that the revealed outputs leak limited information about the private training data.

4.2 FedST Kernel: Federated Shapelet Search

The transformed data set $\langle D \rangle$ is a common tabular data set with continuous attributes, which can be used in conjunction with any standard classifier. Consequently, any classifier training protocol built for secretly shared data (e.g., [70, 3, 96, 18]) can be seamlessly integrated into our framework. Nevertheless, there exists no protocol that tackles the orthogonal problem of federated shapelet search and data transformation. Further, the data transformation is to compute the distances between each training series and shapelet, which is just a subroutine of the shapelet search. Thus, the key technical challenge within our FedST is to design secure and efficient protocols to achieve the *federated shapelet search* (Stage 1 in Figure 3), which becomes the kernel part of FedST.

Formally, we define the functionality of the federated shapelet search, \mathcal{F}_{FedSS} , as follows.

Definition 3 (Federated shapelet search, \mathcal{F}_{FedSS})

Given the time series datasets distributed over the parties, i.e., TD^0, \dots, TD^{n-1} , and the shapelet candidates \mathcal{SC} generated from TD^0 , the goal of \mathcal{F}_{FedSS} is to search for the K best shapelets $\{S_k | S_k \in \mathcal{SC}\}_{k=1}^K$ for P_0 by leveraging the distributed data sets.

To realize \mathcal{F}_{FedSS} under the security defined in Definition 2, a straightforward thought is to design security protocols by extending the centralized method to the FL setting using MPC. Following this, we present $\Pi_{FedSS-B}$ (Section 5.1), the protocol that achieves our basic idea. We show the protocol is *secure* and *effective* (Section 5.2), but we identify that it suffers from

low efficiency due to the high communication overhead incurred by MPC and the failure of the pruning techniques due to the security issue (Section 5.3).

To tackle the efficiency issue, we propose *secure acceleration techniques tailored for the FL setting* that dramatically boost the protocol efficiency by optimizing the two bottlenecked processes of $\Pi_{FedSS-B}$, i.e., the *distance computation* (Section 6) and the *quality measurement* (Section 7). Experiment results show that each of these techniques is *individually effective* and they together contribute to **three orders of magnitude of speedup** (Section 8.3).

Besides, since the evaluation of each shapelet candidate is in a randomized order and independent from the others, FedSS can perform in an anytime fashion [6, 33]. That is, the user announces a time contract, so that the evaluation stops once the running time exceeds the contract, and only the assessed candidates are considered in the following steps. Since this strategy relies only on the publicly available running time, it is feasible in the FL setting [53] to flexibly balance the accuracy and efficiency. We verify this issue in Section 8.5.

5 Basic protocol $\Pi_{FedSS-B}$

We now introduce the basic protocol $\Pi_{FedSS-B}$, which is extended from the centralized shapelet search using MPC to protect the intermediate information (Section 5.1). We discuss the protocol in terms of security, effectiveness, and efficiency in Section 5.2, and analyze the bottlenecks of the protocol in Section 5.3.

5.1 Protocol Description

$\Pi_{FedSS-B}$ is outlined in Algorithm 1. The parties jointly assess the quality of each candidate and then select the K best as the shapelets. The algorithm performs in three steps. First, the parties compute the distance between the samples and each candidate (Lines 2-8). Second, the parties evaluate the quality of the candidate over the secretly shared distances and labels (Lines 9). Finally, the parties jointly retrieve the K candidates with the highest quality and reveal the shares of the indices to P_0 to recover the selected shapelets (Lines 10-11). These three steps are described as follows.

Distance Computation. Since the candidates are locally generated by P_0 , the distance between the samples of P_0 and the candidates can be locally computed. After that, P_0 secretly shares the results to enable the subsequent steps (Lines 3-5).

Algorithm 1: Basic Protocol $\Pi_{FedSS-B}$

Input: $TD^i = \{(T_j^i, y_j^i)\}_{j=1}^{M_i}$, $i = 0, \dots, n-1$: local datasets
 SC : A set of shapelet candidates locally generated by P_0
 K : the number of shapelets
Output: $\{S_k\}_{k=1}^K$: shapelets revealed to P_0

```

1 for  $S \in SC$  do
2   for  $i \in \{0, \dots, n-1\}$  do
3     if  $i == 0$  then
4       for  $j \in \{1, \dots, M_0\}$  do
5          $P_0$  locally computes  $d_{T_j^0, S}$  and
           secretly shares the result among all
           parties
6       else
7         for  $j \in \{1, \dots, M_i\}$  do
8           All parties jointly compute  $\langle d_{T_j^i, S} \rangle$ 
9   All parties jointly compute the quality  $\langle Q_{IG}(S) \rangle$ 
           over the secretly shared distances and labels
10  All parties jointly find the  $K$  candidates with the
           highest quality and reveal the indices  $\{I_k\}_{k=1}^K$ 
           to  $P_0$ 
11 return  $\{S_k = SC_{I_k}\}_{k=1}^K$ 

```

To compute the distances between the samples of each participant P_i and the candidates (Lines 6-8), the MPC operations have to be adopted. For example, to compute $d_{T_j^i, S}$, P_i and P_0 secretly share T_j^i and S respectively. Next, the parties jointly compute each Euclidean norm $\langle \|S, T_j^i[p, L]\|^2 \rangle$ using MPC. At last, the parties jointly determine the shapelet distance $\langle d_{T_j^i, S} \rangle$ by Eq. 2 using the secure minimum operation (see Section 3.3).

Quality Measurement. Based on Eq 3, to compute the IG quality of $S \in SC$ (Line 9), we need to securely partition the dataset D_S using each threshold τ and compute the number of samples belonging to each class c ($c \in \{1, \dots, C\}$) for D_S , $D_S^{\tau, L}$, and $D_S^{\tau, R}$. We achieve it over the secretly shared distances and labels by leveraging the *indicating vector* defined as follows.

Definition 4 (Indicating Vector) Given a dataset $D = \{x_j\}_{j=1}^M$ and a subset $A \subseteq D$, we define the indicating vector of A , denoted as $\gamma_{A \subseteq D}$, as a vector of size M whose j -th ($j \in \{1, \dots, M\}$) entry represents whether x_j is in A , i.e., $\gamma_{A \subseteq D}[j] = 1$ if $x_j \in A$, and 0 otherwise.

For example, for $D = \{x_1, x_2, x_3\}$ and $A = \{x_1, x_3\}$, the indicating vector of A is $\gamma_{A \subseteq D} = (1, 0, 1)$. Suppose that $\gamma_{A_1 \subseteq D}$ and $\gamma_{A_2 \subseteq D}$ are the indicating vectors of A_1 and A_2 , respectively, we have

$$\gamma_{A_1 \subseteq D} \cdot \gamma_{A_2 \subseteq D} = |A_1 \cap A_2|, \quad (8)$$

where $|A_1 \cap A_2|$ is the cardinality of $A_1 \cap A_2$. Specifically, we have $\gamma_{A_1 \subseteq D} \cdot \mathbf{1} = |A_1|$.

With the indicating vector, we securely compute $\langle Q_{IG}(S) \rangle$ as follows.

At the beginning, P_0 generates a vector of size C to indicate the class of S , i.e.,

$$\gamma_{y(S)} = \gamma_{\{y(S)\} \subseteq \{c\}_{c=1}^C}, \quad (9)$$

and secretly shares the vector among all parties.

Next, for each splitting threshold

$$\langle \tau \rangle \in \bigcup_{i=0}^{n-1} \{\langle d_{T_j^i, S} \rangle\}_{j=1}^{M_i}, \quad (10)$$

the parties jointly compute the secretly shared vector

$$\langle \gamma_L \rangle = \langle \gamma_{D_S^{\tau, L} \subseteq D_S} \rangle, \quad (11)$$

$$\langle \gamma_R \rangle = \langle \gamma_{D_S^{\tau, R} \subseteq D_S} \rangle = \mathbf{1} - \langle \gamma_L \rangle,$$

where

$$\langle \gamma_{D_S^{\tau, L} \subseteq D_S}[j] \rangle = \langle d_{T_j^i, S} \rangle < \langle \tau \rangle, \quad j \in \{1, \dots, M\}. \quad (12)$$

Meanwhile, each party P_i secretly shares the vector $\gamma_{TD_c^i \subseteq TD^i}$ to indicate its samples that belong to each class c . Denote the indicating vectors of all parties as

$$\langle \gamma_c \rangle = (\langle \gamma_{TD_c^0 \subseteq TD^0} \rangle, \dots, \langle \gamma_{TD_c^{n-1} \subseteq TD^{n-1}} \rangle), \quad (13)$$

which indicates the samples in D_S that belong to class c , i.e.,

$$\langle \gamma_c \rangle = \langle \gamma_{TD_c \subseteq TD} \rangle = \langle \gamma_{D_{S,c} \subseteq D_S} \rangle. \quad (14)$$

As such, the parties compute the following statistics using MPC:

$$\begin{aligned} \langle |DS_{\tau, L}| \rangle &= \langle \gamma_L \rangle \cdot \mathbf{1}, \\ \langle |DS_{\tau, R}| \rangle &= |DS| - \langle |DS_{\tau, L}| \rangle, \\ \langle |D_{S, y(S)}| \rangle &= \langle \gamma_{y(S)} \rangle \cdot (\langle \gamma_1 \rangle \cdot \mathbf{1}, \dots, \langle \gamma_C \rangle \cdot \mathbf{1}), \\ \langle |D_{S, y(S)}^{\tau, L}| \rangle &= \langle \gamma_{y(S)} \rangle \cdot (\langle \gamma_1 \rangle \cdot \langle \gamma_L \rangle, \dots, \langle \gamma_C \rangle \cdot \langle \gamma_L \rangle), \\ \langle |D_{S, y(S)}^{\tau, R}| \rangle &= \langle \gamma_{y(S)} \rangle \cdot (\langle \gamma_1 \rangle \cdot \langle \gamma_R \rangle, \dots, \langle \gamma_C \rangle \cdot \langle \gamma_R \rangle). \end{aligned} \quad (15)$$

Given the statistics in Equation 15 and the public value $|DS| = M$, the parties can jointly compute $\langle Q_{IG}(S) \rangle$ by Eq. 3.

Shapelet Retrieval. Given the quality of the candidates in secret shares, the parties jointly retrieve the indices of the K best shapelets (Line 10) by securely comparing the adjacent quality values and then swapping the values and the corresponding indices based on the comparison results (see Section 3.3). The indices are output to P_0 to recover the jointly selected shapelets (Line 11).

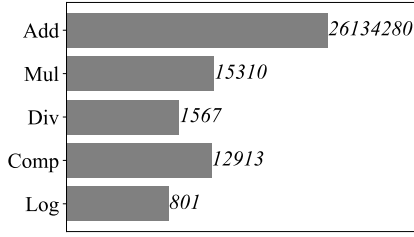


Fig. 4: Throughputs (#operations per second) of different MPC operations executed by three parties. Secure addition is much more efficient than the others because it is executed without communication [15].

5.2 Protocol Discussion

This section analyzes $\Pi_{FedSS-B}$ in terms of security, effectiveness, and efficiency.

Security. The security of $\Pi_{FedSS-B}$ is guaranteed by the following Theorem:

Theorem 1 $\Pi_{FedSS-B}$ is secure under the security defined in Definition 2.

Proof (Proof Sketch) In $\Pi_{FedSS-B}$, all joint computations are executed using MPC. With the indicating vector, the secure computations are data-oblivious. An adversary learns no additional information. The security follows.

Effectiveness. We discuss the protocol effectiveness in terms of classification accuracy. $\Pi_{FedSS-B}$ is directly extended from the centralized approach by using the secret-sharing-based MPC operations, which have considerable computation precision [15, 14, 4]. Therefore, it is expected that the accuracy of FedST has no difference from the centralized approach. The experiment results in Section 8.2 validate this issue.

Efficiency. As shown in Figure 4, the secret-sharing-based MPC is usually bottlenecked by communication rather than computation. Therefore, *it is more indicative to analyze the efficiency by considering the complexity of only the interactive operations*, including the secure multiplication, division, comparison, and logarithm operations. We follow this metric for efficiency analysis in the paper.

$\Pi_{FedSS-B}$ in Algorithm 1 takes $O(|\mathcal{SC}| \cdot MN^2)$ for distance computation. The quality measurement has a complexity of $O(|\mathcal{SC}| \cdot M^2)$. Securely finding the top- K candidates has a complexity of $O(|\mathcal{SC}| \cdot K)$. Since K is usually a small constant, the total complexity of $\Pi_{FedSS-B}$ can be simplified as $O(|\mathcal{SC}| \cdot (MN^2 + M^2))$.

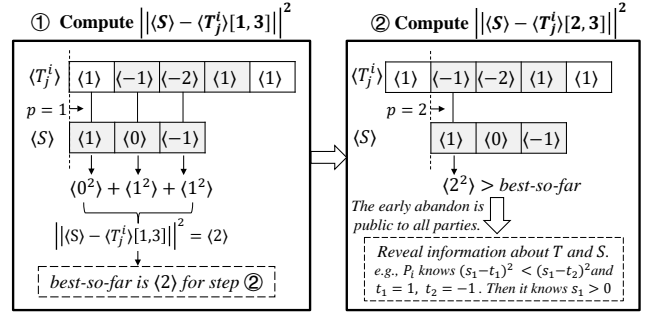


Fig. 5: Illustration of the Euclidean norm pruning and its information disclosure.

5.3 Bottleneck Analysis

As discussed in Section 5.2, $\Pi_{FedSS-B}$ is secure and effective to enable federated shapelet search. However, the basic protocol has expensive time cost in the FL setting for both *distance computation* and *quality measurement* steps, which bottleneck the efficiency of the protocol. Two major reasons are as below.

Reason I. Heavy Communication Overhead. As discussed in Section 5.2, $\Pi_{FedSS-B}$ takes $O(|\mathcal{SC}| \cdot MN^2)$ and $O(|\mathcal{SC}| \cdot M^2)$ expensive interactive operations to compute the distance and measure the quality for all candidates, which dominate in the complexity. Therefore, the efficiency of $\Pi_{FedSS-B}$ is bottlenecked by the first two steps, i.e., distance computation and quality measurement.

Reason II. Failure of Acceleration Techniques. Even using only local computation, repeatedly computing the distance and quality for all candidates are time-consuming [93]. To tackle this, existing studies propose pruning strategies for acceleration [72, 43, 93, 77]. Unfortunately, the pruning techniques are inevitably *data-dependent*, which violates the security of Definition 2 that requires the federated computation oblivious. Thus, we have to abandon these acceleration strategies in the FL setting. We show the security issue in Theorem 2 and Theorem 3.

Theorem 2 Protocol $\Pi_{FedSS-B}$ is insecure under the security defined in Definition 2 if using the Euclidean norm pruning strategies proposed in [43] and [77].

Proof (Proof Sketch) Figure 5 illustrates the Euclidean norm pruning. The basic idea is to maintain a best-so-far Euclidean norm at each timestamp $p \in \{1, \dots, N - L_S + 1\}$, and incrementally compute the sum of the squared differences between each pair of data points when computing $\|S - T_j^i[p, L_S]\|^2$ (left). Once the sum

exceeds the best-so-far value, the current norm computation can be pruned (right). In the FL setting, although we can incrementally compute the sum and compare it with the best-so-far value using MPC, the comparison result must be disclosed when determining the pruning, which cannot be achieved by the simulator \mathcal{S} that attacks the ideal interaction \mathcal{F}_{FedSS} in Definition 3. The security is violated.

Similarly, We have the following theorem.

Theorem 3 *Protocol $\Pi_{FedSS-B}$ is insecure under the security defined in Definition 2 if using the IG quality pruning strategies proposed in [93] and [72].*

We omit the proof because it is similar to the proof of Theorem 2.

Optimizations. To remedy the efficiency issue of the protocol $\Pi_{FedSS-B}$, we propose *acceleration methods tailored for the FL setting* to improve the efficiency of the distance computation and the quality measurement steps.

For distance computation, we propose to speed up the bottlenecked Euclidean norm computation based on a *novel secure dot-product protocol* (Section 6).

For quality measurement, we first propose a *secure sorting-based acceleration* to reduce the duplicated interactive operations for computing IG (Section 7.1). Then, we propose to *tap an alternative F-stat measure* to further improve the efficiency with comparable accuracy (Section 7.2).

Experiment results show that each of these three techniques is individually effective and they together brings up to *three orders of magnitude of speedup* to $\Pi_{FedSS-B}$. Further, compared to our well-optimized IG, the F-stat-based method in Section 7.2 gives 1.04-8.31x of speedup while guaranteeing *no statistical difference* in TSC accuracy. (Section 8.3).

6 Shapelet Distance Acceleration

In $\Pi_{FedSS-B}$, the distance between a candidate S and the $M - M_0$ samples $T_j^i (\forall j, i \neq 0)$ is straightforwardly computed using MPC. Based on Eq 2, the interactive operations used include:

1. $L_S(N - L_S + 1)(M - M_0)$ pairwise multiplications for the Euclidean norm;
2. $(N - L_S + 1)(M - M_0)$ times of both comparisons and assignments for the minimum.

Because the shapelet length L_S is up to N where $N \gg 1$, the efficiency is dominated by the Euclidean norm. Thus, it is necessary to accelerate the distance

Algorithm 2: The Two-Party Dot-Product Protocol of [38]

Input: $\mathbf{x} \in \mathbb{R}^L$ from P_0 ; $\mathbf{y} \in \mathbb{R}^L$ from P_i
($i \in \{1, \dots, n-1\}$)

Output: β to P_0 and α to P_i , satisfying
 $\beta - \alpha = \mathbf{x}^T \cdot \mathbf{y}$

- 1 **Party P_0** randomly chooses \mathbf{Q} , r , \mathbf{f} , R_1 , R_2 , R_3 , \mathbf{x}_i ($i \in \{1, \dots, d\}, i \neq r$) and creates \mathbf{X} . Then, it computes b , \mathbf{U} , \mathbf{c} , \mathbf{g} , and sends \mathbf{U} , \mathbf{c} , \mathbf{g} to P_i
 - 2 **Party P_i** randomly chooses α , creates \mathbf{y}' , computes and sends to P_0 the value a , h
 - 3 **Party P_0** computes β
-

computation by improving the efficiency of the bottlenecked *Euclidean norm*.

The work of [38] proposes a two-party dot-product protocol (as Algorithm 2) that we find is both computation and communication efficient for the calculation between one vector and many others. It motivates us that we can compute the Euclidean norm between a candidate S and the total $(N - L_S + 1)(M - M_0)$ subseries of the participants using the dot-product protocol. Unfortunately, the protocol in Algorithm 2 (denoted as the raw protocol) has weak security that violates Definition 2.

To overcome the limitation, we propose Π_{DP} , a *secure dot-product protocol* that enhances the raw protocol using MPC. We prove that this novel protocol not only follows the security of Definition 2, but also effectively accelerates the Euclidean norm. We describe the acceleration method in Section 6.1. Then, we analyze the security deficiency of the raw protocol and propose our Π_{DP} in Section 6.2.

6.1 Dot-Product-based Euclidean Norm

Given two vectors $\mathbf{x} \in \mathbb{R}^L$ from P_0 and $\mathbf{y} \in \mathbb{R}^L$ from P_i , Algorithm 2 computes the dot-product $\mathbf{x} \cdot \mathbf{y}$ as follows.

(i) P_0 chooses a random matrix $\mathbf{Q} \in \mathbb{R}^{d \times d}$ ($d \geq 2$), a random value $r \in \{1, \dots, d\}$, a random vector $\mathbf{f} \in \mathbb{R}^{L+1}$ and three random values R_1, R_2, R_3 , and selects $s - 1$ random vectors

$$\mathbf{x}_i \in \mathbb{R}^{L+1}, i \in \{1, \dots, r-1, r+1, \dots, d\}. \quad (16)$$

Next, it creates a matrix

$$\mathbf{X} \in \mathbb{R}^{d \times (L+1)}, \quad (17)$$

whose i -th row ($i \neq r$) is \mathbf{x}_i and r -th row is

$$\mathbf{x}'^T = (x_1, \dots, x_L, 1). \quad (18)$$

Then, P_0 locally computes

$$b = \sum_{j=1}^d \mathbf{Q}_{j,r}, \quad (19)$$

$$\mathbf{U} = \mathbf{Q} \cdot \mathbf{X}, \quad (20)$$

$$\mathbf{c} = \sum_{i \in \{1, \dots, d\}, i \neq r} (\mathbf{x}_i^T \cdot \sum_{j=1}^d \mathbf{Q}_{j,i}) + R_1 R_2 \mathbf{f}^T, \quad (21)$$

$$\mathbf{g} = R_1 R_3 \mathbf{f}. \quad (22)$$

Finally, it sends \mathbf{U} , \mathbf{c} , \mathbf{g} to P_i (Line 1);

(ii) P_i chooses a random value α to generate

$$\mathbf{y}' = (y_1, \dots, y_L, \alpha)^T. \quad (23)$$

Next, it computes and sends to P_0 two scalars a and h (Line 2), as:

$$a = \sum_{j=1}^d \mathbf{U}_j \cdot \mathbf{y}' - \mathbf{c} \cdot \mathbf{y}', \quad (24)$$

$$h = \mathbf{g}^T \cdot \mathbf{y}'. \quad (25)$$

(iii) P_0 locally computes β (Line 3) as:

$$\beta = \frac{a}{b} + \frac{hR_2}{bR_3}. \quad (26)$$

Given β and α , the result satisfies $\mathbf{x}^T \cdot \mathbf{y} = \beta - \alpha$.

The *Euclidean norm computation* in our federated shapelet search can benefit from the above protocol, since each $\|S, T_j^i[p, L_S]\|^2$ can be represented as

$$\begin{aligned} \|S, T_j^i[p, L_S]\|^2 &= \sum_{p'=1}^{L_S} (s_{p'})^2 + \sum_{p'=1}^{L_S} (t_{p'+p-1})^2 \\ &\quad + 2 \sum_{p'=1}^{L_S} s_{p'} t_{p'+p-1}, \end{aligned} \quad (27)$$

where the term

$$z = \sum_{p'=1}^{L_S} s_{p'} t_{p'+p-1} = \mathbf{S}^T \cdot \mathbf{T}_j^i[\mathbf{p}, \mathbf{L}_S] \quad (28)$$

can be computed by P_0 and P_i jointly executing the protocol to get β and α , respectively. The terms $\sum_{p'=1}^{L_S} (s_{p'})^2$ and $\sum_{p'=1}^{L_S} (t_{p'+p-1})^2$ can be locally computed by the two parties. To this end, all parties aggregate the three

Algorithm 3: Secure Dot-Product Protocol

 Π_{DP} (Ours)

Input: $\mathbf{x} \in \mathbb{R}^L$ from P_0 ; $\mathbf{y} \in \mathbb{R}^L$ from P_i
($i \in \{1, \dots, n-1\}$)

Output: $\langle z \rangle$ secretly shared by all parties, satisfying
 $z = \mathbf{x}^T \cdot \mathbf{y}$

- 1 **Party P_0** and **Party P_i** represent each element of their input vectors as fixed-point number encoded in \mathbb{Z}_q as used in MPC
 - 2 **Party P_0** independently and randomly chooses each value of \mathbf{Q} , \mathbf{f} , R_1 , R_2 , R_3 , \mathbf{x}_i ($i \in \{1, \dots, d\}, i \neq r$) from \mathbb{Z}_q , $r \in \{1, \dots, d\}$, creates \mathbf{X} , computes b , \mathbf{U} , \mathbf{c} , \mathbf{g} , and sends \mathbf{U} , \mathbf{c} , \mathbf{g} to P_i .
 - 3 **Party P_i** randomly chooses $\alpha \in \mathbb{Z}_q$, creates \mathbf{y}' , and computes the value a , h . Then, P_i sends only h to P_0
 - 4 **All Parties jointly compute**
 $\langle z \rangle = \langle \beta \rangle - \langle \alpha \rangle = \langle \frac{1}{b} \rangle \cdot \langle a \rangle + \langle \frac{hR_2}{bR_3} \rangle - \langle \alpha \rangle$ using MPC
-

terms in secret shares using non-interactive secure addition.

Using the above dot-product protocol, the total communication cost for the $(N - L_S + 1)(M - M_0)$ Euclidean norm between S and the subseries of the participants is reduced from $O(L_S(N - L_S + 1)(M - M_0))$ to $O(L_S) + O((N - L_S + 1)(M - M_0))$.

6.2 Security Analysis and Enhancement

Although the protocol in Algorithm 2 benefits the efficiency of the distance computation, it is unavailability due to the security issue.

Theorem 4 *The protocol of Algorithm 2 is insecure under the security defined in Definition 2.*

Proof (Proof Sketch) Consider an adversary \mathcal{A} that attacks P_0 . By executing the raw protocol in Algorithm 2, \mathcal{A} receives the messages a and h . For ease of exposition, we represent the matrix \mathbf{U} as a row of the column vectors, i.e.,

$$\mathbf{U} = (\mathbf{u}_1, \dots, \mathbf{u}_{L+1}), \quad (29)$$

where

$$\mathbf{u}_i = (\mathbf{U}_{1,i}, \dots, \mathbf{U}_{d,i})^T, i \in \{1, \dots, L+1\}. \quad (30)$$

Denote

$$\mathbf{c} = (c_1, \dots, c_{L+1}) \quad (31)$$

and

$$\mathbf{g}^T = (g_1, \dots, g_{L+1}). \quad (32)$$

Recall that $\mathbf{v}' = (\mathbf{v}^T, \alpha)^T$. Thus, it has

$$a = \sum_{j=1}^d \mathbf{U}_j \cdot \mathbf{v}' - \mathbf{c} \cdot \mathbf{v}' = \mathbf{e}_1^T \cdot \mathbf{v} + w\alpha, \quad (33)$$

$$h = \mathbf{g}^T \cdot \mathbf{v}' = \mathbf{e}_2^T \cdot \mathbf{v} + g_{L+1}\alpha, \quad (34)$$

where

$$\mathbf{e}_1 = \left(\sum \mathbf{u}_1 + c_1, \dots, \sum \mathbf{u}_L + c_L \right)^T, \quad (35)$$

$$w = \left(\sum \mathbf{u}_{L+1} + c_{L+1} \right), \quad (36)$$

$$\mathbf{e}_2 = (g_1, \dots, g_L)^T. \quad (37)$$

Based on Eq 33-34, \mathcal{A} knows that

$$g_{L+1}a - wh = (g_{L+1}\mathbf{e}_1^T - w\mathbf{e}_2^T) \cdot \mathbf{v}, \quad (38)$$

where $g_{L+1}\mathbf{e}_1^T - w\mathbf{e}_2^T$ is created locally in P_0 . Obviously, the probability distribution of $g_{L+1}a - wh$ is dependent on the private data \mathbf{v} , which cannot be simulated by any \mathcal{S} .

Our novel protocol Π_{DP} . To securely achieve the acceleration, we propose Π_{DP} , a novel dot-product protocol that follows the security in Definition 2. The basic idea is to enhance the security of Algorithm 2 using MPC and the finite field arithmetic. This solution is simple but rather effective in terms of both security and efficiency.

Π_{DP} is presented in Algorithm 3. It has three differences to the raw protocol:

1. P_0 and P_i represent each element of their input vectors as fixed-point number encoded in \mathbb{Z}_q as used in MPC [15,14,4] (Line 1), generates each random masking value from the same field \mathbb{Z}_q , and compute b , \mathbf{U} , \mathbf{c} , \mathbf{g} , and a , h in \mathbb{Z}_q [15] (Lines 2-3);
2. P_i only sends h to P_0 but keeps a private (Line 3);
3. the value $\beta - \alpha$ is jointly computed by all parties using MPC (Line 4).

Note that the protocol incurs only one additional interactive operation when computing $\langle z \rangle = \langle \frac{1}{b} \rangle \langle a \rangle$. Thus, computing the Euclidean norm between S and the $M - M_0$ series requires still $O(L_S) + O((N - L_S + 1)(M - M_0))$, which is *much smaller* compared to the directly using of the MPC operations in $\Pi_{FedSS-B}$.

More importantly, we verify the security guarantee of Π_{DP} .

Theorem 5 Π_{DP} is secure under the security definition defined in Definition 2.

Proof (Proof Sketch) Since the secretly-sharing-based MPC are secure, we focus on the messages beyond it. We describe two simulators \mathcal{S}_0 and \mathcal{S}_i that simulate the messages of the adversaries for party P_0 and P_i , respectively.

We first present \mathcal{S}_0 . Similar to Eq 34, when receiving the message h , the adversary knows

$$h = (\mathbf{e}_2^T \cdot \mathbf{v} + g_{L+1}\alpha) \bmod q \quad (39)$$

Since the masking values \mathbf{e}_2^T , g_{L+1} , and α are independently and uniformly sampled from \mathbb{Z}_q , the distribution of h is equal to $h' = g_{L+1}\alpha \bmod q$. In the ideal interaction, \mathcal{S}_0 independently and randomly chooses α and g_{L+1} from \mathbb{Z}_q to compute and send h' to the adversary. Indeed the views of the environment in both ideal and real interactions are indistinguishable.

Next, we discuss \mathcal{S}_i . By executing Π_{DP} in the real interaction, the adversary of P_i receives \mathbf{U} , \mathbf{c} , \mathbf{g} . Both \mathbf{c} and \mathbf{g} are derived from independent and randomly chosen values. Thus, \mathcal{S}_i can follow the same procedure to compute them. Without loss of generality, we assume $r = 1$ and $d = 2$. Then, $\mathbf{U} = \mathbf{Q} \cdot \mathbf{X}$ follows

$$\begin{pmatrix} \mathbf{Q}_{1,1}x_1 + \mathbf{Q}_{1,2}x_{2,1} & \mathbf{Q}_{2,1}x_1 + \mathbf{Q}_{2,2}x_{2,1} \\ \dots & \dots \\ \mathbf{Q}_{1,1}x_L + \mathbf{Q}_{1,2}x_{2,L} & \mathbf{Q}_{2,1}x_L + \mathbf{Q}_{2,2}x_{2,L} \\ \mathbf{Q}_{1,1} + \mathbf{Q}_{1,2}x_{2,L+1} & \mathbf{Q}_{2,1} + \mathbf{Q}_{2,2}x_{2,L+1} \end{pmatrix}^T \quad (40)$$

Note that we omit the modular operations at each entry for ease of exposition. The value of each entry is masked by a unique triplet, e.g., $(\mathbf{Q}_{11}, \mathbf{Q}_{12}, \mathbf{x}_{21})$ at the entry (1,1). Because the values of these triplets are independently and randomly chosen from \mathbb{Z}_q , the elements of \mathbf{U} are independent and identically distributed. Similar to \mathcal{S}_0 , \mathcal{S}_i can simulate \mathbf{U} by computing \mathbf{U}' , where

$$\mathbf{U}'_{i,j} = \mathbf{Q}_{i,k}x_{i,j} \bmod q, \quad k \in \{1, \dots, d\}, \quad (41)$$

and sends it along with \mathbf{c} , \mathbf{g} to the adversary. The views of the environment in both ideal and real interaction are identically distributed.

In summary, the simulators achieve the same effect that the adversaries achieve. The security follows.

With the security guarantee, we can integrate Π_{DP} into $\Pi_{FedSS-B}$ to accelerate the distance computation. The protocol Π_{DP} can also serve as a building block for other applications.

7 Quality Measurement Acceleration

Empirically, evaluating the shapelet quality using IG with the binary strategy (Section 3.2) is the state-of-the-art method in terms of TSC accuracy. However, computing IG in the FL setting suffers from a severe efficiency issue. The reasons are concluded as follows.

1. A large number (M) of thresholds will be evaluated for each candidate;
2. Evaluating different thresholds incurs duplicated interactive operations;
3. Evaluating one threshold is already inefficient mainly because the required secure division and logarithm operations are expensive (as illustrated in Figure 4);
4. The IG pruning strategies lose their efficacy due to the security issue (Section 5.3).

To consider both accuracy and efficiency, we propose to speed up the quality measurement in $\Pi_{FedSS-B}$ in two aspects:

O1: Accelerating IG computation. To benefit from IG in terms of TSC accuracy, we propose a speed-up method to reduce as many interactive operations as possible in computing IG based on *secure sorting* (Section 7.1), which tackles the problem in reason 1.

O2: Tapping alternative measures. As the problems of 1, 3 and 4 are the *inherent deficiencies* of IG which is difficult to avoid, we propose a trade-off method tailored for the FL setting by tapping other measures that are much more secure-computation-efficient than IG, at the cost of acceptable loss of TSC accuracy (Section 7.2).

7.1 Sorting-based IG Acceleration

The straightforward IG computation in Section 5.1 is inefficient since it incurs $O(M^2)$ *secure comparisons* for $\langle \gamma_L \rangle$, and $O(M^2)$ *secure multiplications* for $\langle |DS_{\tau,L,y(S)}| \rangle$ and $\langle |DS_{\tau,R,y(S)}| \rangle$. Inspired by [72] and [3], we propose to securely reduce the duplicated interactive operations by pre-sorting the secretly shared distances and labels before computing each $Q_{IG}(S)$.

Assuming $\langle DS \rangle = \bigcup_{i=0}^{n-1} \{ \langle d_{T_j^i, S} \rangle \}_{j=1}^{M_i}$ are arranged in an *ordered sequence*, i.e.,

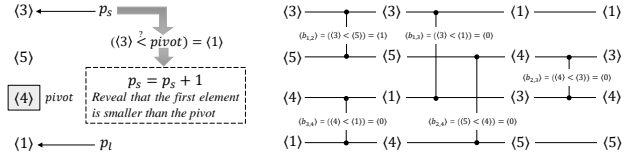
$$\langle D'_S \rangle = \{ \langle d_j \rangle \}_{j=1}^M, \quad (42)$$

where

$$d_{j_1} < d_{j_2}, \forall 1 \leq j_1 < j_2 \leq M. \quad (43)$$

As such, for each threshold $\langle \tau \rangle = \langle d_j \rangle$, we can get γ'_L without using secure comparison, as:

$$\gamma'_L = \gamma_{DS'_{\tau,L} \subseteq DS'} \quad (44)$$



(a) Example of Quicksort. The elements should be partitioned based on whether they are smaller than the pivot or not. Even performed in secret shares, the process will disclose the order information about the input.

(b) The sorting network of size 4 used to sort the sequence. It contains 5 comparison operations which are determined only by the network size. Thus, by extending the sorting network using the secure comparison and assignment protocols, both the value and the order information can be protected.

Fig. 6: Running examples of sorting the sequence ($\langle 3 \rangle$, $\langle 5 \rangle$, $\langle 4 \rangle$, $\langle 1 \rangle$) using Quicksort and the sorting network.

where

$$\gamma'_L[j'] = \begin{cases} 1, & j' < j \\ 0, & \text{otherwise} \end{cases} \quad (45)$$

Meanwhile, if $\langle \gamma_c \rangle (c \in \{1, \dots, C\})$ is permuted into $\langle \gamma'_c \rangle$ such that for each entry j' , $\langle \gamma'_c \rangle$ and $\langle D'_S \rangle$ indicates the same sample, i.e.,

$$\langle \gamma'_c \rangle[j'] = \langle \gamma_{TD_c^i \subseteq TD^i} \rangle[j] \iff \langle d_{j'} \rangle = \langle d_{T_j^i, S} \rangle, \quad (46)$$

we can compute the statistics in Eq. 15 by replacing $\langle \gamma_L \rangle$, $\langle \gamma_R \rangle$, $\langle \gamma_c \rangle$ with γ'_L , $\gamma'_R = \mathbf{1} - \gamma'_L$, $\langle \gamma'_c \rangle$, respectively. Note that the newly produced γ'_L is in plaintext thanks to the order of $\langle DS' \rangle$. Thus, it requires only $O(C)$ secure multiplications to compute the statistics in Eq 15 for each threshold, where C is a small constant representing the number of classes.

Based on the above observation, the key to the acceleration is to *securely sort* the secretly shared *distances* and the *indicating vectors* of the class labels. Note that to satisfy the security in Definition 2, no any intermediate information can be disclosed during the federated sorting, including not only the secretly shared values but also their order.

Although we can protect each of the values using MPC, the common sorting algorithms, e.g., Quicksort or Merge sort, rely on the *order information* of the sort keys to reduce complexity. As a result, the order information will be disclosed during their running, which violates the security in Definition 2. We take the Quicksort as an example to illustrate the leakage of the order information, as is shown in Figure 6a.

To address the security problem while achieving a complexity smaller than $O(M^2)$, we adopt the sorting network [8] to securely sort the distances. Given an input size, the sorting network has a *fixed order of comparison operations*, regardless of the order of the input

sequence [8]. Therefore, we can protect both the value and the order information by *performing the comparison and swapping operations using the secure comparison and assignment protocols* (see Section 3.3) respectively. Figure 6b is a running example of combining the sorting network and the MPC protocols.

The distances $\langle D_S \rangle$ is taken as the sorting key to permute both $\langle D_S \rangle$ and $\langle \gamma_c \rangle$ ($c \in \{1, \dots, C\}$) consistently. The output corresponds to the assumption in Equation 42-43 and 46. The sorting network takes $O(M \log^2 M)$ interactive operations for the input of size M [8]. Thus, the complexity of computing each $\langle Q_{IG}(S) \rangle$ becomes $O(M \log^2 M)$, which is much smaller than the $O(M^2)$ in $\Pi_{FedSS-B}$.

Theorem 6 *The sorting-based acceleration is secure under the security definition defined in Definition 2.*

Proof (Proof Sketch) The main difference between the acceleration method and the basic protocol for the IG computation is the usage of the sorting network, which is proved to be data-oblivious [10]. Thus, the security of the sorting-based acceleration follows.

7.2 Alternative-Measures-based Trade-off

As discussed at the beginning of Section 7, although IG-based method is superior in TSC accuracy, it is naturally difficult to efficiently compute this metric. To further accelerate the quality measure step, we propose to tap *alternative measures* that can be securely and more efficiently achieved in the FL setting, while guaranteeing comparable TSC accuracy.

The shapelet quality can be evaluated by other measures, such as Kruskal-Wallis (KW) [54], Mood's Median (MM) [54], and ANOVA F (F-stat) test [35]. However, these quality measures are less considered in recent works [12, 6, 68], since they have no significant advantage over IG in terms of both accuracy and efficiency, especially when the binary strategy [12] and the IG pruning technique [72] are integrated. In the brand new FL scenario, the *expensive communication cost* incurred by interactive operations and the *failure of the pruning* for computing IG remind us to reexamine these alternatives.

F-stat-based quality measurement. As shown in [35], using F-stat for TSC slightly outperforms the methods with KW and MM in terms of accuracy. More essentially, F-stat performs with $O(M)$ secure multiplications and $C+1$ secure divisions in the FL setting, while both KW and MM require $O(M \log^2 M)$ secure comparison and assignment operations because they rely on secure sorting, and they also need C times of divisions.

Thus, we choose F-stat as the alternative measure to achieve the trade-off.

Given $D_S = \{d_{T_j, S}\}_{j=1}^M$ and $\{y_j\}_{j=1}^M$ where $y_j \in \{c\}_{c=1}^C$, the F-stat is defined as:

$$Q_F(S) = \frac{\sum_{c=1}^C (\bar{D}_{S,c} - \bar{D}_S)^2 / (C-1)}{\sum_{c=1}^C \sum_{y_j=c} (d_{T_j, S} - \bar{D}_{S,c})^2 / (M-C)}, \quad (47)$$

where $\bar{D}_{S,c} = \frac{\sum_{d \in D_{S,c}} d}{|D_{S,c}|}$ is the mean distance w.r.t. class c with $D_{S,c} = \{d_{T_j, S} | y_j = c\}_{j=1}^M$, and \bar{D}_S is the mean of all distances.

Similar to the IG computing in Section 5.1, we leverage the *indicating vector* to indicate whether each sample belongs to each of the C classes. Given

$$\langle D_S \rangle = \bigcup_{i=0}^{n-1} \{\langle d_{T_j^i, S} \rangle\}_{j=1}^{M_i}, \quad (48)$$

and the indicating vector $\langle \gamma_c \rangle$ ($c \in \{1, \dots, C\}$) as:

$$\langle \gamma_c \rangle = (\langle \gamma_{TD^0 \subseteq TD^0}^0 \rangle, \dots, \langle \gamma_{TD^{n-1} \subseteq TD^{n-1}}^{n-1} \rangle), \quad (49)$$

the parties jointly compute the terms:

$$\begin{aligned} \langle \bar{D}_{S,c} \rangle &= \frac{\langle \mathbf{D}_S \rangle \cdot \langle \gamma_c \rangle}{\langle \gamma_c \rangle \cdot \mathbf{1}}, c \in \{1, \dots, C\} \\ \langle \bar{D}_S \rangle &= \frac{\langle \mathbf{D}_S \rangle \cdot \mathbf{1}}{M}. \end{aligned} \quad (50)$$

Next, they jointly compute:

$$\sum_{y_j=c} (d_{T_j, S} - \bar{D}_{S,c})^2 = \langle \mathbf{d}_c \rangle \cdot \langle \mathbf{d}_c \rangle, c \in \{1, \dots, C\}, \quad (51)$$

where

$$\langle \mathbf{d}_c \rangle[j] = \langle \gamma_c \rangle[j] \cdot (\langle d_{T_j, S} \rangle - \bar{D}_{S,c}), j \in \{1, \dots, M\}. \quad (52)$$

Then, the parties can jointly compute $\langle Q_F(S) \rangle$ by Equation 47.

The protocol for $\langle Q_F(S) \rangle$ has a complexity of $O(M)$, while the computation of $\langle Q_{IG}(S) \rangle$ using our optimization in Section 7.1 still takes $O(M \log^2 M)$ interactive operations. Moreover, the empirical evaluation in Section 8.3 shows that the F-stat-based FedST achieves comparable accuracy to the prior IG-based solution.

Theorem 7 *The F-stat-based shapelet quality measurement is secure under the security definition defined in Definition 2.*

Proof (Proof Sketch) Similar to the IG-based method in Section 5.1 and Section 7.1, the input and output of the F-stat are both secret shares. The MPC operations and indicating vectors are used to make the computation data-oblivious. The security follows.

8 Experiments

In this section, we empirically evaluate the effectiveness of the FedST method and the acceleration techniques.

8.1 Experimental Setup

Our experimental setups are as follows:

Implementation. FedST is implemented in Python. We utilize the SPDZ library [41] for semi-honest additive-secret-sharing-based MPC. The security parameter is $\kappa = 40$, which ensures that the probability of information leakage, i.e., the quantity in Definition 2 is less than $2^{-\lambda}$ ($\lambda = \kappa$) [15, 14].

Environment. We build a cross-silo federated learning environment by running parties in isolated 16G RAM and 8 core Platinum 8260 CPUs docker containers installed with Ubuntu 20.04 LTS. The parties communicate with each other through the docker bridge network with 4Gbps bandwidth.

Datasets. We use both the *real-world datasets* and the *synthetic datasets* for evaluation at the following two different scales.

To evaluate the effectiveness of FedST framework, we use the popular 117 fixed-length TSC datasets of the UCR Archive [21] that are collected from different types of applications, such as ECG or motion recognition. In the cross-silo and horizontal setting, each business has considerable (but still insufficient) training samples for every class. Thus, we randomly partition the training samples into 3 equal-size subsets to ensure each party has at least two samples for each class. Since there are 20 small datasets that cannot be partitioned as above, we omit them and test on the remaining 97 datasets.

To investigate the effectiveness of the acceleration techniques, we first assess the efficiency improvement of these techniques using the synthetic datasets. Since the secure computation is data-independent, we randomly generate the synthetic datasets of varying parameters. Next, we compare the F-stat to the prior IG measure in terms of both accuracy and efficiency on the 97 UCR datasets to validate the effectiveness of the trade-off.

Metrics. We use the *accuracy* to evaluate the classification, which is measured as the number of samples that are correctly predicted over the testing dataset. For efficiency, we measure the *running time* of the protocols in each step.

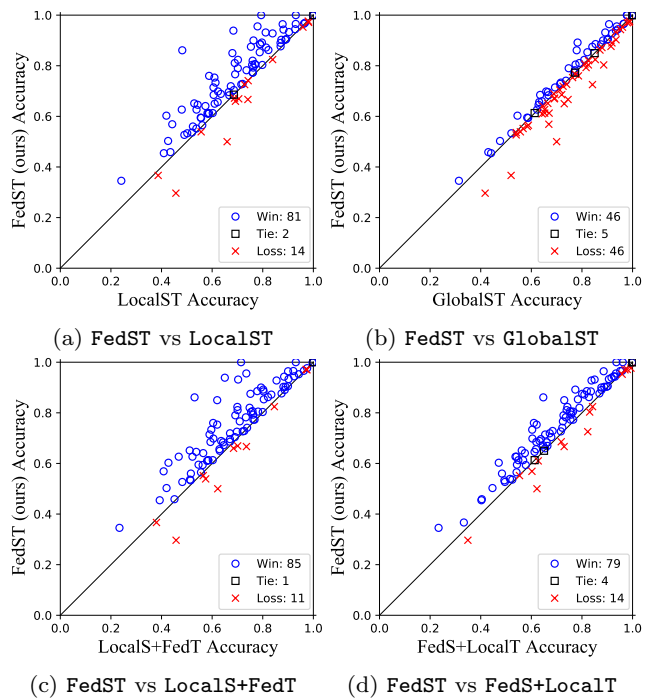


Fig. 7: Pairwise comparison between FedST and the baselines on 97 UCR datasets. The blue/black/red scatters represent the datasets where FedST wins/ties/loses the competitors.

8.2 Effectiveness of the FedST Framework

Baselines. Since the advantage of the shapelet transformation against other TSC methods has been widely shown [7, 6, 68], we focus on investigating the *effectiveness of enabling FL for TSC* in terms of classification accuracy. To achieve this goal, we compare our FedST with the four baselines:

- **LocalST:** the currently available solution that P_0 performs the centralized shapelet transformation with only its own data;
- **GlobalST:** the ideal solution that P_0 uses the data of all parties for centralized shapelet transformation without privacy protection;
- **LocalS+FedT:** a variant of FedST that P_0 executes the shapelet search step locally and collaborates with the participants for federated data transformation and classifier training;
- **FedS+LocalT:** a variant of FedST that P_0 locally performs data transformation and classifier training using the shapelets found through federated shapelet search.

Following the centralized setting [6, 35], we adopt random forest as the classifier over the transformed data for all the methods. The candidates are sampled with the length ranging from $\min(3, \frac{N}{4})$ to N . The candidate set size is $\frac{MN}{2}$ and number of shapelets K is set

to $\min\{\frac{N}{2}, 200\}$ and is reduced to 5 by clustering the found shapelets. The prior IG is used for assessing the shapelet quality.

Pairwise comparison. Figure 7 reports the pairwise accuracy comparison of our FedST against the competitors.

Figure 7a shows that FedST is more accurate than the LocalST on most of the datasets. It indicates the effectiveness of our basic idea of enabling FL to improve the TSC accuracy. Figure 7b shows that FedST achieves accuracy close to the non-private GlobalST, which coincides with our analysis in Section 5.2. The slight difference can be caused by two reasons. First, the global method samples the shapelets from all data, while in FedST the candidates are only generated by P_0 for the interpretability constraints. Second, in secret sharing, the float values are encoded in fixed-point representation for efficiency, which results in the truncation. Fortunately, we show later in Figure 8 that there is *no statistically significant difference* in accuracy between FedST and GlobalST. From Figure 7c and Figure 7d, we can see that both the variants are much worse than FedST. It means that both the stages of FedST are indispensable.

Multiple comparisons. We present the critical difference diagram [23] of the methods in Figure 8. It reports the *mean ranking of accuracy* among the 97 UCR datasets. The competitors falling in one clique (the bold horizontal line) have no statistical difference, while the opposite for the methods from different cliques. Figure 8 shows that FedST is *no statistically different* from GlobalST and they both statistically significantly outperforms LocalST. It is notable that the variant conducting only local shapelet search (LocalS+FedT), even using all parties’ data for transformation, is slightly inferior to LocalST. The reason could be that the locally selected shapelets have poor quality due to the lack of training data, which may cause the transformed data to be more misleading to degrade the accuracy. In comparison, FedS+LocalT performs better than LocalST, because the shapelet quality is improved by FL with more training data used for shapelet search. Both variants are much inferior to FedST, which indicates the positive effect of FL for both stages.

8.3 Effectiveness of the Acceleration Techniques

Efficiency improvement. To assess the effectiveness of the proposed acceleration approaches, we first investigate their *efficiency improvement* using the synthetic datasets of varying dataset size (M), time series length (N), number of parties (n) and candidate set size $|SC|$.

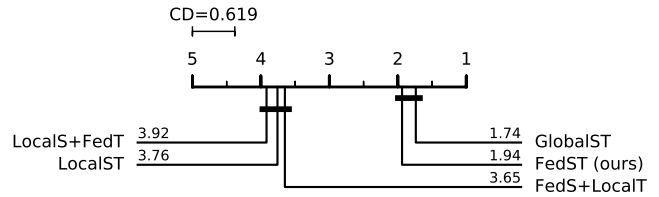


Fig. 8: Critical difference diagram for our FedST and the baselines under the statistical level of 0.05.

The average length of the shapelet candidates and the number of shapelets (K) are fixed to the moderate values of $0.6N$ and 200, respectively. Overall, the results presented in Figure 9 coincide with our complexity analysis.

1) Distance computation. Figure 9a-9c report the time of computing the shapelet distance between a candidate S and all training samples T_j^i w.r.t. M , N , and n . The time for both $\Pi_{FedSS-B}$ that directly uses MPC (d -MPC) and the optimization leveraging the proposed secure dot-product protocol (d -MPC+ Π_{DP}) scale linearly to M and n . However, d -MPC+ Π_{DP} can achieve up to 30x of speedup over d -MPC for the default $N = 100$. The time of d -MPC increases more quickly than d -MPC+ Π_{DP} as N increases, because the complexity of d -MPC is quadratic w.r.t. N while our proposed d -MPC+ Π_{DP} has a linear complexity of interactive operations.

We also show the time of finding the minimum Euclidean norm (Find-Min), which is a subroutine of the shapelet distance computation. The results show that Find-Min is much faster than d -MPC, which is consistent with our analysis in Section 6 that the time of d -MPC is dominated by the *Euclidean norm computation*. In comparison, the time of d -MPC+ Π_{DP} is very close to the time of Find-Min because the Euclidean norm computation time is substantially reduced (more than 58x speedup) with our Π_{DP} .

2) Quality measurement. We show the time of quality measurement for each candidate S with varying M and n in Figure 9d-9e. Compared to the IG computation in the basic protocol (Q_{IG}), our proposed secure-sorting-based computation (Q_{IG} + $Sorting$) achieves a similar performance when M is small, but the time of Q_{IG} increases much faster than Q_{IG} + $Sorting$ as M increases because Q_{IG} has a quadratic complexity to M . In comparison, the time of Q_{IG} + $Sorting$ is dominated by the secure sorting protocol ($Sorting$), which has a complexity of $O(M \log^2 M)$. The optimized Q_{IG} + $Sorting$ is also more scalable to n than Q_{IG} .

Using F-stat in the quality measurement step (Q_F) can achieve more than 65x of speedup over the optimized Q_{IG} + $Sorting$. It is also noteworthy that Q_F is much faster than $Sorting$ which bottlenecks the time

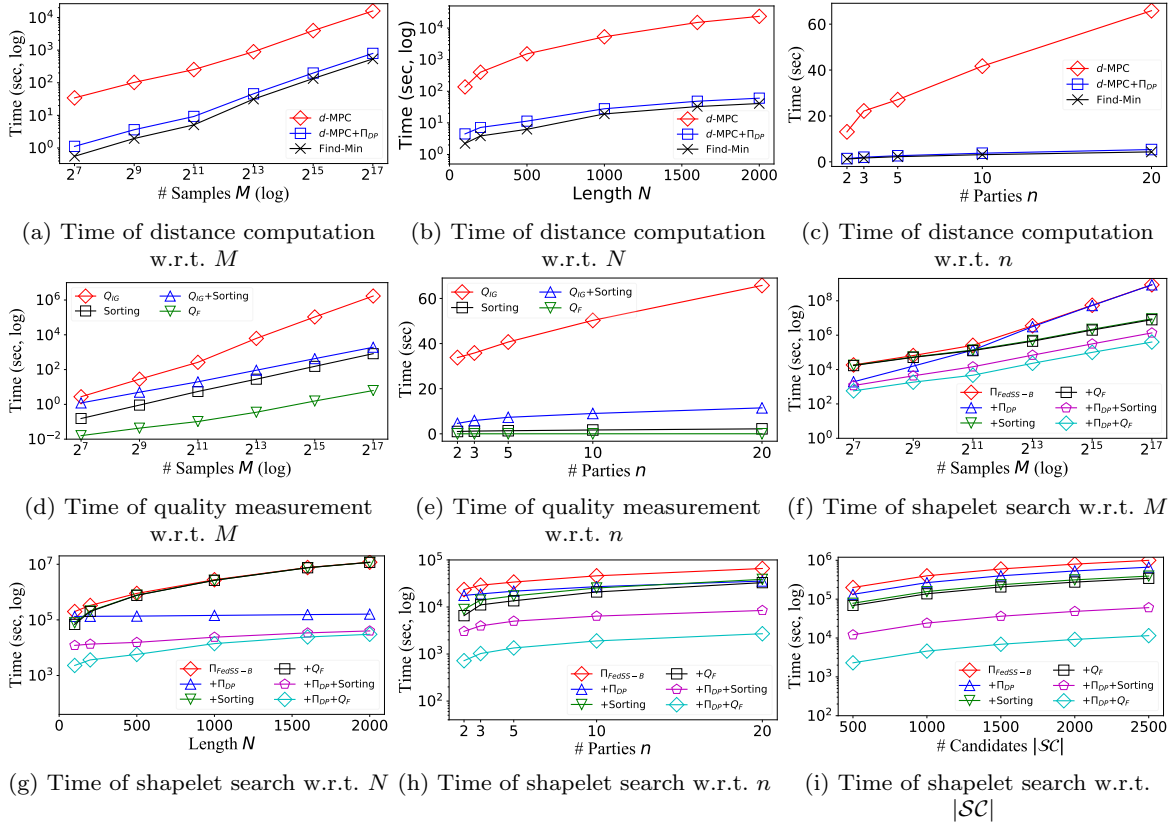


Fig. 9: Performance of varying dataset size M (default 512), series length N (default 100), number of parties n (default 3), and candidate set size $|SC|$ (default 500).

of securely computing the KW and MM, as mentioned in Section 7.2. That is why we consider the F-stat for the acceleration.

3) Federated shapelet search. Finally, we assess the *total running time of the federated shapelet search protocol* with each proposed acceleration technique. The results are reported in Figure 9f-9i.

Overall, an individual Π_{DP} -based acceleration ($+\Pi_{DP}$) brings 1.01-73.59x of improvement over $\Pi_{FedSS-B}$. The sorting-based ($+Sorting$) technique gives 1.01-96.17x of speedup alone and the F-stat-based method ($+Q_F$) individually achieves 1.01-107.76x of speedup. The combination of these techniques is always more effective than each individual. Π_{DP} -based and Sorting-based methods together ($+\Pi_{DP}+Sorting$) contribute 15.12-630.97x of improvement, while the combination of the Π_{DP} -based and F-stat-based techniques ($+\Pi_{DP}+Q_F$) boosts the protocol efficiency by 32.22-2141.64x.

We notice from Figure 9f that the time of $\Pi_{FedSS-B}$ is dominated by the distance computation when M is small. In this case, $+\Pi_{DP}$ is more effective. With the increase of M , the quality measurement step gradually dominates the efficiency. As a result, the $+Sorting$ and $+Q_F$ play a more important role in acceleration. Simi-

larly, Figure 9g shows that the efficiency is dominated by the quality measurement when N is small and is gradually dominated by the distance computation with N increases. The acceleration techniques for these two steps are always complementary with each other.

It is also worth noting that the time of all competitors is nearly *in direct proportion to* $|SC|$, as shown in Figure 9i. The result is consistent with our analysis in Section 5.2 that the time for securely *finding the top- K candidates* (Algorithm 1 Line 10), which has a complexity of $O(K \cdot |SC|)$, is *negligible* compared to the time of distance computation and quality measurement. That is why we mainly dedicate to accelerating these two steps.

Effectiveness of the trade-off strategy. We investigate the effectiveness of the F-stat-based protocol in *trading off TSC accuracy and the protocol efficiency*. Specifically, we evaluate both the accuracy and the federated shapelet search time for the two versions of FedST that adopt either the prior Q_{IG} (FedST- Q_{IG}) or the more efficient Q_F (FedST- Q_F). The experiments are conducted using 97 UCR datasets with the same setting as Section 8.2. Both the Π_{DP} -based and the sorting-based speedup methods are adopted.

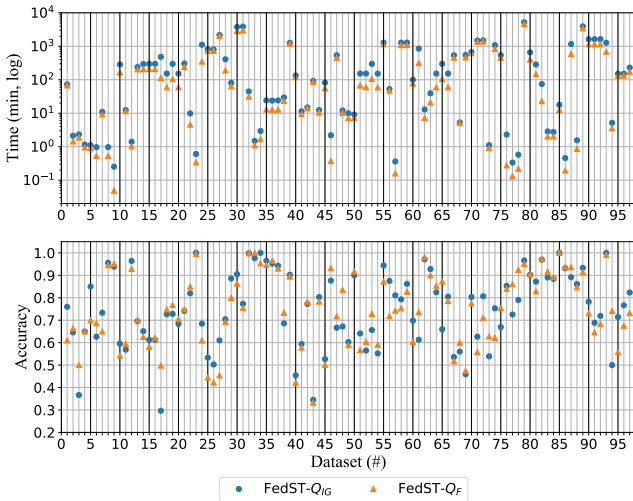


Fig. 10: Accuracy and federated shapelet search time of FedST using different quality measures.

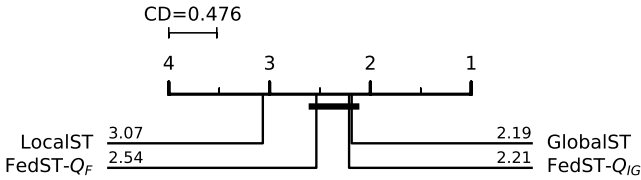
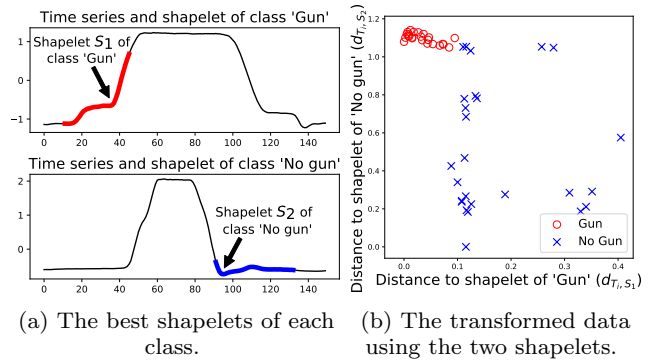


Fig. 11: Critical difference diagram for FedST that uses different quality measures and the two baselines. The statistical level is 0.05.

As shown in Figure 10 top, FedST-Q_F is faster than FedST-Q_{IG} on all 97 datasets. The efficiency improvement is 1.04-8.31x while the average speedup on the 97 datasets is 1.79x. Meanwhile, FedST-Q_F is better than FedST-Q_{IG} on 41 of the 97 datasets in terms of accuracy (Figure 10 bottom). The average accuracy of FedST-Q_F is just 0.5% lower than that of FedST-Q_{IG}. Figure 11 shows the critical difference diagram for these two methods and the two FL baselines (LocalST and GlobalST). The result indicates that FedST-Q_F achieves the same level of accuracy as FedST-Q_{IG} and GlobalST, and is significantly better than LocalST. In summary, our proposed F-stat-based trade-off strategy can effectively improve the efficiency of the federated shapelet search while guaranteeing comparable accuracy to the superior IG-based method.

8.4 Study of Interpretability

Figure 12 demonstrates the interpretability of FedST using a real-world motion classification problem named GunPoint [21]. The data track the centroid of the actors’ right hand for two types of motions. For “Gun”



(a) The best shapelets of each class. (b) The transformed data using the two shapelets.

Fig. 12: Interpretability study using GunPoint [21].

class, they draw a replicate gun from a hip-mounted holster, point it at a target, then return the gun to the holster and their hands to their sides. For “No gun (Point)”, the actors have their gun by their sides, point with their index fingers to a target, and then return their hands. The best shapelets of the two classes are shown in Figure 12a, which are derived from the data of the initiator and represent the class-specific features, i.e., the hand tracks of drawing the gun (S_1) and putting down the hand (S_2). We transform all time series samples into the distances to these shapelets and visualize the results in Figure 12b. As can be seen, instead of considering the original time series space which has 150 data points per sample, by using the two shapelets, the classification can be explained with the concise rule that the samples more similar to S_1 and distant from S_2 belong to class “Gun” (red), and the opposite for the “No gun” data (blue). The study indicates that the shapelet-based features are easier to interpret than the raw time series.

8.5 Study of Flexibility

We further investigate the flexibility of FedST as discussed in Section 4.2. We evaluate the accuracy and the protocol running time on each of the 97 UCR datasets with the time contract varying from 10% to 90% of the maximum running time (the time evaluated in Section 8.3 using IG). Figure 13 reports the results. Overall, the accuracy increases with more time is allowed, while the real running time is always close to the contract. It validates the effectiveness of balancing the accuracy and efficiency using the user-defined time contract, which is beneficial for the practical utility.

Note that with only 10% running time (approximate 10% candidates assessed at random), FedST can achieve at least 77% of the maximum accuracy among the 97 datasets, which implies that the high-quality

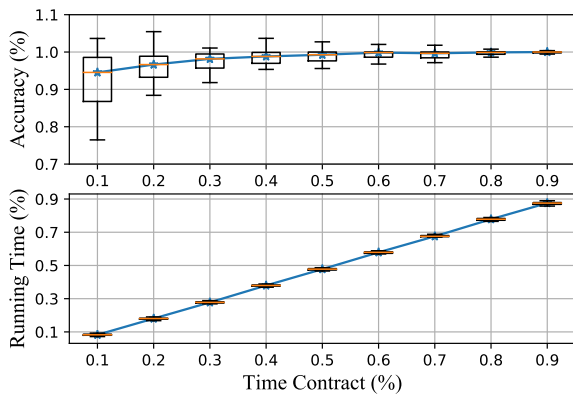


Fig. 13: The accuracy (top) and real running time (bottom) w.r.t. the user-defined time contract.

shapelets are highly redundant. The results also confirm the feasibility of generating candidates from P_0 in the cross-silo setting where each party has considerable (but insufficient) data.

9 Further Enhancement by Incorporating Differential Privacy

As discussed in Section 4.1, FedST allows only the found shapelets and the learned models to be revealed to the initiator P_0 . In this section, we illustrate that we can incorporate differential privacy (DP) [26] for additional privacy protection, guaranteeing that the released shapelets and models disclose limited information about the private training data of the parties. The differential privacy is defined as follows.

Definition 5 (Differential Privacy) Formally, a function f satisfies (ϵ, δ) -DP, if for any two data sets D and D' differing in a single record and any output O of f , we have

$$\Pr[f(D) \in O] \leq e^\epsilon \cdot \Pr[f(D') \in O] + \delta, \quad (53)$$

where ϵ is the privacy budget controlling the tradeoff between the accuracy of f and the degree of privacy protection that f offers.

Intuitively, the function f is differentially private since the probability of producing a given output (e.g., shapelets or models) is not highly dependent on whether a particular data record exists in D . As a result, the information about each private record cannot be inferred from the output with a high probability.

In FedST, we have two main stages: the federated shapelet search that produces the K best shapelets, and the data transformation and classifier training step which builds the classification model and outputs the

model parameters. Many existing works have studied DP algorithms to protect the parameters of the commonly used models [89, 1, 16], which can be seamlessly integrated into FedST. Therefore, we elaborate below on how to incorporate DP to the federated shapelet search.

As defined in Definition 3, the federated shapelet search takes the parties' training time series data and the shapelet candidates as the input, and the output is the K candidates with the highest quality (Q_{IG} or Q_F depending on the used measure). Note that the quality of each candidate is evaluated using all training time series samples. Therefore, we can keep the private training samples from being disclosed by *protecting the quality of each individual candidate*. To achieve this goal, we make the quality of the candidates *noisy* before retrieving the K best ones.

Concisely, the parties jointly add secretly shared noises to the quality of all candidates using the secure random number generator [41]. The noise for each candidate should be identically and independently distributed and follows a Laplace distribution whose parameter is public and related to ϵ , which is referred to as the *Laplace mechanism* [26]. To this end, the parties retrieve the candidate with the *maximum* quality by executing the secure comparison and assignment protocols (see Section 3.3) and reveal the index to P_0 . The two steps are repeated K times to find the noisy K best shapelets.

The above algorithm for finding the maximum is referred to as the *Report Noisy Max* algorithm [26], which is $(\epsilon, 0)$ -differentially private. Thus, according to Theorem 3 in [25], the algorithm of retrieving the K best shapelet candidates by calling the Report Noisy Max algorithm is (ϵ', δ') -DP for any $\delta' \geq 0$ where

$$\epsilon' = \min \left\{ \epsilon K, \epsilon K \left(\frac{e^\epsilon - 1}{e^\epsilon + 1} \right) + \sqrt{2\epsilon^2 K \ln\left(\frac{1}{\delta'}\right)} \right\}. \quad (54)$$

In conclusion, the integration of DP provides an additional layer to protect the privacy of the revealed shapelets and models, which can further enhance the security of FedST.

10 Conclusion and future works

This work studies how to customize federated learning solution for the time series classification problem. We systematically investigate existing TSC methods for the centralized scenario and propose FedST, a novel FL-enabled TSC framework based on the centralized shapelet transformation. We design the security protocol $\Pi_{FedSS-B}$ for the FedST kernel, analyze its effec-

tiveness, and identify its efficiency bottlenecks. To accelerate the protocol, we propose specific optimizations tailored for the FL setting. Both theoretical analysis and experiment results show the effectiveness of our proposed FedST framework and the acceleration techniques.

In the future, we would like to consider other types of interpretable features to complement FedST. Further, we wish to develop high-performance system to support industrial-scale applications.

References

- Abadi, M., Chu, A., Goodfellow, I., McMahan, H.B., Mironov, I., Talwar, K., Zhang, L.: Deep learning with differential privacy. In: Proceedings of the 2016 ACM SIGSAC conference on computer and communications security, pp. 308–318 (2016)
- Abanda, A., Mori, U., Lozano, J.A.: A review on distance based time series classification. *Data Mining and Knowledge Discovery* **33**(2), 378–412 (2019)
- Abspoel, M., Escudero, D., Volgushev, N.: Secure training of decision trees with continuous attributes. *Cryptology ePrint Archive* (2020)
- Aly, A., Smart, N.P.: Benchmarking privacy preserving scientific operations. In: International Conference on Applied Cryptography and Network Security, pp. 509–529. Springer (2019)
- Aono, Y., Hayashi, T., Trieu Phong, L., Wang, L.: Scalable and secure logistic regression via homomorphic encryption. In: Proceedings of the Sixth ACM Conference on Data and Application Security and Privacy, pp. 142–144 (2016)
- Bagnall, A., Flynn, M., Large, J., Lines, J., Middlehurst, M.: A tale of two toolkits, report the third: on the usage and performance of hive-cote v1. 0. *arXiv e-prints* pp. arXiv-2004 (2020)
- Bagnall, A., Lines, J., Bostrom, A., Large, J., Keogh, E.: The great time series classification bake off: a review and experimental evaluation of recent algorithmic advances. *Data Mining and Knowledge Discovery* **31**, 606–660 (2017)
- Batcher, K.E.: Sorting networks and their applications. In: Proceedings of the April 30–May 2, 1968, spring joint computer conference, pp. 307–314 (1968)
- Beaver, D.: Efficient multiparty protocols using circuit randomization. In: Annual International Cryptology Conference, pp. 420–432. Springer (1991)
- Bogdanov, D., Laur, S., Talviste, R.: A practical analysis of oblivious sorting algorithms for secure multi-party computation. In: Nordic Conference on Secure IT Systems, pp. 59–74. Springer (2014)
- Bonawitz, K., Ivanov, V., Kreuter, B., Marcedone, A., McMahan, H.B., Patel, S., Ramage, D., Segal, A., Seth, K.: Practical secure aggregation for privacy-preserving machine learning. In: proceedings of the 2017 ACM SIGSAC Conference on Computer and Communications Security, pp. 1175–1191 (2017)
- Bostrom, A., Bagnall, A.: Binary shapelet transform for multiclass time series classification. In: Transactions on Large-Scale Data-and Knowledge-Centered Systems XXXII, pp. 24–46. Springer (2017)
- Cabello, N., Naghizade, E., Qi, J., Kulik, L.: Fast and accurate time series classification through supervised interval search. In: 2020 IEEE International Conference on Data Mining (ICDM), pp. 948–953. IEEE (2020)
- Catrina, O., Hoogh, S.d.: Improved primitives for secure multiparty integer computation. In: International Conference on Security and Cryptography for Networks, pp. 182–199. Springer (2010)
- Catrina, O., Saxena, A.: Secure computation with fixed-point numbers. In: International Conference on Financial Cryptography and Data Security, pp. 35–50. Springer (2010)
- Chaudhuri, K., Monteleoni, C.: Privacy-preserving logistic regression. *Advances in neural information processing systems* **21** (2008)
- Chen, J., Zhang, A.: Fedmsplit: Correlation-adaptive federated multi-task learning across multimodal split networks. In: Proceedings of the 28th ACM SIGKDD Conference on Knowledge Discovery and Data Mining, pp. 87–96 (2022)
- Chen, V., Pastro, V., Raykova, M.: Secure computation for machine learning with spdz. *arXiv preprint arXiv:1901.00329* (2019)
- Cheng, K., Fan, T., Jin, Y., Liu, Y., Chen, T., Papadopoulos, D., Yang, Q.: Secureboost: A lossless federated learning framework. *IEEE Intelligent Systems* **36**(6), 87–98 (2021)
- Damgård, I., Pastro, V., Smart, N., Zakarias, S.: Multiparty computation from somewhat homomorphic encryption. In: Annual Cryptology Conference, pp. 643–662. Springer (2012)
- Dau, H.A., Bagnall, A.J., Kamgar, K., Yeh, C.M., Zhu, Y., Gharghabi, S., Ratanamahatana, C.A., Keogh, E.J.: The UCR time series archive. *CoRR* **abs/1810.07758** (2018). URL <http://arxiv.org/abs/1810.07758>
- Dempster, A., Schmidt, D.F., Webb, G.I.: Minirocket: A very fast (almost) deterministic transform for time series classification. In: Proceedings of the 27th ACM SIGKDD conference on knowledge discovery & data mining, pp. 248–257 (2021)
- Demšar, J.: Statistical comparisons of classifiers over multiple data sets. *The Journal of Machine learning research* **7**, 1–30 (2006)
- Dheepadharshani, S., Anandh, S., Bhavinaya, K., Lavanya, R.: Multivariate time-series classification for automated fault detection in satellite power systems. In: 2019 International Conference on Communication and Signal Processing (ICCSP), pp. 0814–0817. IEEE (2019)
- Durfee, D., Rogers, R.M.: Practical differentially private top-k selection with pay-what-you-get composition. In: H. Wallach, H. Larochelle, A. Beygelzimer, F. d'Alché-Buc, E. Fox, R. Garnett (eds.) *Advances in Neural Information Processing Systems*. Curran Associates, Inc.
- Dwork, C., Roth, A., et al.: The algorithmic foundations of differential privacy. *Foundations and Trends® in Theoretical Computer Science* **9**(3–4), 211–407 (2014)
- Fang, W., Zhao, D., Tan, J., Chen, C., Yu, C., Wang, L., Wang, L., Zhou, J., Zhang, B.: Large-scale secure xgb for vertical federated learning. In: Proceedings of the 30th ACM International Conference on Information & Knowledge Management, pp. 443–452 (2021)
- Fang, Z., Wang, P., Wang, W.: Efficient learning interpretable shapelets for accurate time series classification. In: 2018 IEEE 34th International Conference on Data Engineering (ICDE), pp. 497–508. IEEE (2018)
- Fu, F., Shao, Y., Yu, L., Jiang, J., Xue, H., Tao, Y., Cui, B.: Vf2boost: Very fast vertical federated gradient

- boosting for cross-enterprise learning. In: Proceedings of the 2021 International Conference on Management of Data, pp. 563–576 (2021)
30. Fu, F., Xue, H., Cheng, Y., Tao, Y., Cui, B.: Blindfl: Vertical federated machine learning without peeking into your data. In: Proceedings of the 2022 International Conference on Management of Data, pp. 1316–1330 (2022)
 31. Ghalwash, M.F., Radosavljevic, V., Obradovic, Z.: Extraction of interpretable multivariate patterns for early diagnostics. In: 2013 IEEE 13th International Conference on Data Mining, pp. 201–210. IEEE (2013)
 32. Goldreich, O., Oren, Y.: Definitions and properties of zero-knowledge proof systems. *Journal of Cryptology* **7**(1), 1–32 (1994)
 33. Gordon, D., Hendler, D., Rokach, L.: Fast randomized model generation for shapelet-based time series classification. arXiv preprint arXiv:1209.5038 (2012)
 34. Grabocka, J., Schilling, N., Wistuba, M., Schmidt-Thieme, L.: Learning time-series shapelets. In: Proceedings of the 20th ACM SIGKDD international conference on Knowledge discovery and data mining, pp. 392–401. ACM (2014)
 35. Hills, J., Lines, J., Baranauskas, E., Mapp, J., Bagnall, A.: Classification of time series by shapelet transformation. *Data mining and knowledge discovery* **28**(4), 851–881 (2014)
 36. Hou, L., Kwok, J.T., Zurada, J.M.: Efficient learning of timeseries shapelets. In: Thirtieth Aaai conference on artificial intelligence (2016)
 37. Huang, Y., Chu, L., Zhou, Z., Wang, L., Liu, J., Pei, J., Zhang, Y.: Personalized cross-silo federated learning on non-iid data. In: AAAI, pp. 7865–7873 (2021)
 38. Ioannidis, I., Grama, A., Atallah, M.: A secure protocol for computing dot-products in clustered and distributed environments. In: Proceedings International Conference on Parallel Processing, pp. 379–384. IEEE (2002)
 39. Ismail Fawaz, H., Forestier, G., Weber, J., Idoumghar, L., Muller, P.A.: Deep learning for time series classification: a review. *Data mining and knowledge discovery* **33**(4), 917–963 (2019)
 40. Kairouz, P., McMahan, H.B., Avent, B., Bellet, A., Bennis, M., Bhagoji, A.N., Bonawitz, K., Charles, Z., Cormode, G., Cummings, R., et al.: Advances and open problems in federated learning. *Foundations and Trends® in Machine Learning* **14**(1–2), 1–210 (2021)
 41. Keller, M.: Mp-spdz: A versatile framework for multiparty computation. In: Proceedings of the 2020 ACM SIGSAC conference on computer and communications security, pp. 1575–1590 (2020)
 42. Keller, M., Scholl, P., Smart, N.P.: An architecture for practical actively secure mpc with dishonest majority. In: Proceedings of the 2013 ACM SIGSAC conference on Computer & communications security, pp. 549–560 (2013)
 43. Keogh, E., Wei, L., Xi, X., Lee, S.H., Vlachos, M.: Lb.keogh supports exact indexing of shapes under rotation invariance with arbitrary representations and distance measures. In: Proceedings of the 32nd international conference on Very large data bases, pp. 882–893. Cite-seer (2006)
 44. Large, J., Bagnall, A., Malinowski, S., Tavenard, R.: On time series classification with dictionary-based classifiers. *Intelligent Data Analysis* **23**(5), 1073–1089 (2019)
 45. Le Nguyen, T., Gsponer, S., Ifrim, G.: Time series classification by sequence learning in all-subsequence space. In: 2017 IEEE 33rd international conference on data engineering (ICDE), pp. 947–958. IEEE (2017)
 46. Li, G., Choi, B., Xu, J., Bhowmick, S.S., Chun, K.P., Wong, G.L.H.: Shapenet: A shapelet-neural network approach for multivariate time series classification. In: Proceedings of the AAAI Conference on Artificial Intelligence, vol. 35, pp. 8375–8383 (2021)
 47. Li, L., Fan, Y., Tse, M., Lin, K.Y.: A review of applications in federated learning. *Computers & Industrial Engineering* **149**, 106,854 (2020)
 48. Li, Q., Wen, Z., He, B.: Practical federated gradient boosting decision trees. In: Proceedings of the AAAI conference on artificial intelligence, vol. 34, pp. 4642–4649 (2020)
 49. Li, T., Sahu, A.K., Talwalkar, A., Smith, V.: Federated learning: Challenges, methods, and future directions. *IEEE Signal Processing Magazine* **37**(3), 50–60 (2020)
 50. Li, X., Dowsley, R., De Cock, M.: Privacy-preserving feature selection with secure multiparty computation. In: International Conference on Machine Learning, pp. 6326–6336. PMLR (2021)
 51. Li, Z., Ding, B., Zhang, C., Li, N., Zhou, J.: Federated matrix factorization with privacy guarantee. *Proceedings of the VLDB Endowment* **15**(4), 900–913 (2021)
 52. Liang, Z., Wang, H.: Efficient class-specific shapelets learning for interpretable time series classification. *Information Sciences* **570**, 428–450 (2021)
 53. Liang, Z., Wang, H.: Fedtsc: A secure federated learning system for interpretable time series classification. *Proc. VLDB Endow.* **15**(12), 3686–3689 (2022). DOI 10.14778/3554821.3554875. URL <https://doi.org/10.14778/3554821.3554875>
 54. Lines, J., Bagnall, A.: Alternative quality measures for time series shapelets. In: International Conference on Intelligent Data Engineering and Automated Learning, pp. 475–483. Springer (2012)
 55. Lines, J., Taylor, S., Bagnall, A.: Time series classification with hive-cote: The hierarchical vote collective of transformation-based ensembles. *ACM Transactions on Knowledge Discovery from Data* **12**(5) (2018)
 56. Liu, J., Lou, J., Xiong, L., Liu, J., Meng, X.: Projected federated averaging with heterogeneous differential privacy. *Proceedings of the VLDB Endowment* **15**(4), 828–840 (2021)
 57. Liu, Y., Kang, Y., Xing, C., Chen, T., Yang, Q.: A secure federated transfer learning framework. *IEEE Intelligent Systems* **35**(4), 70–82 (2020)
 58. Liu, Y., Wu, W., Flokas, L., Wang, J., Wu, E.: Enabling sql-based training data debugging for federated learning. *Proc. VLDB Endow.* **15**(3), 388–400 (2021). DOI 10.14778/3494124.3494125. URL <https://doi.org/10.14778/3494124.3494125>
 59. Ma, Q., Zhuang, W., Cottrell, G.: Triple-shapelet networks for time series classification. In: 2019 IEEE International Conference on Data Mining (ICDM), pp. 1246–1251. IEEE (2019)
 60. Ma, Q., Zhuang, W., Li, S., Huang, D., Cottrell, G.: Adversarial dynamic shapelet networks. In: Proceedings of the AAAI Conference on Artificial Intelligence, vol. 34, pp. 5069–5076 (2020)
 61. Mammen, P.M.: Federated learning: opportunities and challenges. arXiv preprint arXiv:2101.05428 (2021)
 62. Marfoq, O., Xu, C., Neglia, G., Vidal, R.: Throughput-optimal topology design for cross-silo federated learning. *Advances in Neural Information Processing Systems* **33**, 19,478–19,487 (2020)
 63. McMahan, B., Moore, E., Ramage, D., Hampson, S., y Arcas, B.A.: Communication-efficient learning of deep

- networks from decentralized data. In: *Artificial intelligence and statistics*, pp. 1273–1282. PMLR (2017)
64. McMahan, H.B., Moore, E., Ramage, D., y Arcas, B.A.: Federated learning of deep networks using model averaging. *arXiv preprint arXiv:1602.05629* **2** (2016)
 65. McMahan, H.B., Ramage, D., Talwar, K., Zhang, L.: Learning differentially private recurrent language models. *arXiv preprint arXiv:1710.06963* (2017)
 66. Middlehurst, M., Large, J., Bagnall, A.: The canonical interval forest (cif) classifier for time series classification. In: *2020 IEEE international conference on big data (big data)*, pp. 188–195. IEEE (2020)
 67. Middlehurst, M., Large, J., Cawley, G., Bagnall, A.: The temporal dictionary ensemble (tde) classifier for time series classification. In: *Machine Learning and Knowledge Discovery in Databases*, pp. 660–676. Springer (2020)
 68. Middlehurst, M., Large, J., Flynn, M., Lines, J., Bostrom, A., Bagnall, A.: Hive-cote 2.0: a new meta ensemble for time series classification. *Machine Learning* **110**(11), 3211–3243 (2021)
 69. Middlehurst, M., Vickers, W., Bagnall, A.: Scalable dictionary classifiers for time series classification. In: *International Conference on Intelligent Data Engineering and Automated Learning*, pp. 11–19. Springer (2019)
 70. Mohassel, P., Zhang, Y.: Secureml: A system for scalable privacy-preserving machine learning. In: *2017 IEEE symposium on security and privacy (SP)*, pp. 19–38. IEEE (2017)
 71. Molnar, C.: *Interpretable Machine Learning*, 2 edn. (2022). URL christophm.github.io/interpretable-ml-book/
 72. Mueen, A., Keogh, E., Young, N.: Logical-shapelets: an expressive primitive for time series classification. In: *Proceedings of the 17th ACM SIGKDD international conference on Knowledge discovery and data mining*, pp. 1154–1162 (2011)
 73. Muhammad, K., Wang, Q., O’Reilly-Morgan, D., Tragos, E., Smyth, B., Hurley, N., Geraci, J., Lawlor, A.: Fedfast: Going beyond average for faster training of federated recommender systems. In: *Proceedings of the 26th ACM SIGKDD International Conference on Knowledge Discovery & Data Mining*, pp. 1234–1242 (2020)
 74. Nikolaenko, V., Weinsberg, U., Ioannidis, S., Joye, M., Boneh, D., Taft, N.: Privacy-preserving ridge regression on hundreds of millions of records. In: *2013 IEEE symposium on security and privacy*, pp. 334–348. IEEE (2013)
 75. Pan, Q., Zhu, Y.: Fedwalk: Communication efficient federated unsupervised node embedding with differential privacy. *Proceedings of the 28th ACM SIGKDD Conference on Knowledge Discovery and Data Mining* (2022)
 76. Pérez-D’Arpino, C., Shah, J.A.: Fast target prediction of human reaching motion for cooperative human-robot manipulation tasks using time series classification. In: *2015 IEEE international conference on robotics and automation (ICRA)*, pp. 6175–6182. IEEE (2015)
 77. Rakthanmanon, T., Campana, B., Mueen, A., Batista, G., Westover, B., Zhu, Q., Zakaria, J., Keogh, E.: Searching and mining trillions of time series subsequences under dynamic time warping. In: *Proceedings of the 18th ACM SIGKDD international conference on Knowledge discovery and data mining*, pp. 262–270 (2012)
 78. Ramirez, E., Wimmer, M., Atzmueller, M.: A computational framework for interpretable anomaly detection and classification of multivariate time series with application to human gait data analysis. In: *Artificial Intelligence in Medicine: Knowledge Representation and Transparent and Explainable Systems*, pp. 132–147. Springer (2019)
 79. Ruiz, A.P., Flynn, M., Large, J., Middlehurst, M., Bagnall, A.: The great multivariate time series classification bake off: a review and experimental evaluation of recent algorithmic advances. *Data Mining and Knowledge Discovery* **35**(2), 401–449 (2021)
 80. Shokri, R., Shmatikov, V.: Privacy-preserving deep learning. In: *Proceedings of the 22nd ACM SIGSAC conference on computer and communications security*, pp. 1310–1321 (2015)
 81. Smith, V., Chiang, C.K., Sanjabi, M., Talwalkar, A.S.: Federated multi-task learning. *Advances in neural information processing systems* **30** (2017)
 82. Susto, G.A., Cenedese, A., Terzi, M.: Time-series classification methods: Review and applications to power systems data. *Big data application in power systems* pp. 179–220 (2018)
 83. Tan, C.W., Dempster, A., Bergmeir, C., Webb, G.I.: Multitrocket: Multiple pooling operators and transformations for fast and effective time series classification. *Data Mining and Knowledge Discovery* pp. 1–24 (2022)
 84. Tang, W., Long, G., Liu, L., Zhou, T., Blumenstein, M., Jiang, J.: Omni-scale cnns: a simple and effective kernel size configuration for time series classification. In: *International Conference on Learning Representations* (2021)
 85. Tong, Y., Pan, X., Zeng, Y., Shi, Y., Xue, C., Zhou, Z., Zhang, X., Chen, L., Xu, Y., Xu, K., et al.: Hu-fu: efficient and secure spatial queries over data federation. *Proceedings of the VLDB Endowment* **15**(6), 1159 (2022)
 86. Voigt, P., Von dem Bussche, A.: *The eu general data protection regulation (gdpr). A Practical Guide*, 1st Ed., Cham: Springer International Publishing **10**(3152676), 10–5555 (2017)
 87. Wang, Y., Tong, Y., Shi, D., Xu, K.: An efficient approach for cross-silo federated learning to rank. In: *2021 IEEE 37th International Conference on Data Engineering (ICDE)*, pp. 1128–1139. IEEE (2021)
 88. Wei, K., Li, J., Ding, M., Ma, C., Yang, H.H., Farokhi, F., Jin, S., Quek, T.Q., Poor, H.V.: Federated learning with differential privacy: Algorithms and performance analysis. *IEEE Transactions on Information Forensics and Security* **15**, 3454–3469 (2020)
 89. Wu, Y., Cai, S., Xiao, X., Chen, G., Ooi, B.C.: Privacy preserving vertical federated learning for tree-based models. *Proceedings of the VLDB Endowment* **13**(11)
 90. Yang, Q., Liu, Y., Chen, T., Tong, Y.: Federated machine learning: Concept and applications. *ACM Transactions on Intelligent Systems and Technology (TIST)* **10**(2), 1–19 (2019)
 91. Yang, S., Ren, B., Zhou, X., Liu, L.: Parallel distributed logistic regression for vertical federated learning without third-party coordinator. *arXiv preprint arXiv:1911.09824* (2019)
 92. Yao, A.C.: Protocols for secure computations. In: *23rd annual symposium on foundations of computer science (sfcs 1982)*, pp. 160–164. IEEE (1982)
 93. Ye, L., Keogh, E.: Time series shapelets: a novel technique that allows accurate, interpretable and fast classification. *Data mining and knowledge discovery* **22**(1-2), 149–182 (2011)
 94. Zhang, C., Li, S., Xia, J., Wang, W., Yan, F., Liu, Y.: {BatchCrypt}: Efficient homomorphic encryption for {Cross-Silo} federated learning. In: *2020 USENIX annual technical conference (USENIX ATC 20)*, pp. 493–506 (2020)

-
95. Zhang, C., Xie, Y., Bai, H., Yu, B., Li, W., Gao, Y.: A survey on federated learning. *Knowledge-Based Systems* **216**, 106,775 (2021)
 96. Zheng, W., Deng, R., Chen, W., Popa, R.A., Panda, A., Stoica, I.: Cerebro: A platform for {Multi-Party} cryptographic collaborative learning. In: 30th USENIX Security Symposium (USENIX Security 21), pp. 2723–2740 (2021)